HHS Public Access

Author manuscript

Cell Rep. Author manuscript; available in PMC 2020 December 03.

Published in final edited form as:

Cell Rep. 2020 November 24; 33(8): 108424. doi:10.1016/j.celrep.2020.108424.

A Two-Step Process of Effector Programming Governs CD4+ T Cell Fate Determination Induced by Antigenic Activation in the Steady State

Adeleye Opejin[1,3], **Alexey Surnov**[1,3], **Ziva Misulovin**[2], **Michelle Pherson**[2], **Cindy Gross**[1], **Courtney A. Iberg**[1], **Ian Fallahee**[1], **Jessica Bourque**[1], **Dale Dorsett**[2], **Daniel Hawiger**[1,4,*]

[1]Department of Molecular Microbiology and Immunology, Saint Louis University School of Medicine, St. Louis, MO, USA

[2]Edward A. Doisy Department of Biochemistry and Molecular Biology, Saint Louis University School of Medicine, St. Louis, MO, USA

[3]These authors contributed equally

[4]Lead Contact

SUMMARY

Various processes induce and maintain immune tolerance, but effector T cells still arise under minimal perturbations of homeostasis through unclear mechanisms. We report that, contrary to the model postulating primarily tolerogenic mechanisms initiated under homeostatic conditions, effector programming is an integral part of T cell fate determination induced by antigenic activation in the steady state. This effector programming depends on a two-step process starting with induction of effector precursors that express Hopx and are imprinted with multiple instructions for their subsequent terminal effector differentiation. Such molecular circuits advancing specific terminal effector differentiation upon re-stimulation include programmed expression of interferon-γ, whose production then promotes expression of T-bet in the precursors. We further show that effector programming coincides with regulatory conversion among T cells sharing the same antigen specificity. However, conventional type 2 dendritic cells (cDC2) and T cell functions of mammalian target of rapamycin complex 1 (mTORC1) increase effector precursor induction while decreasing the proportion of T cells that can become peripheral Foxp3$^+$ regulatory T (pTreg) cells.

*Correspondence: daniel.hawiger@health.slu.edu.

AUTHOR CONTRIBUTIONS

A.O. designed and performed adoptive transfer experiments, EAE experiments, and *in vitro* culture experiments; prepared and analyzed RNA-seq samples; interpreted data; and wrote the manuscript. A.S. designed and performed adoptive transfer experiments and *in vitro* culture experiments, analyzed RNA-seq data, performed GSEA, interpreted data, and wrote the manuscript. A.S., C.G., and A.O. bred and maintained experimental animals. C.A.I. analyzed data. J.B. analyzed data and wrote the manuscript. I.F. produced immunoglobulins. Z.M., M.P., and D.D. performed RNA-seq and ChIP-seq experiments and analysis. All authors contributed to preparing and writing the manuscript. D.H. conceived, designed, and oversaw experiments; interpreted data; and wrote the manuscript.

SUPPLEMENTAL INFORMATION

Supplemental Information can be found online at https://doi.org/10.1016/j.celrep.2020.108424.

DECLARATION OF INTERESTS

The authors declare no competing interests.

In Brief

The mechanisms in the steady state that govern the formation of effector T cells with potentially autoimmune functions remain unclear. Opejin et al. reveal a two-step process starting with induction of effector precursors that express Hopx and are imprinted with multiple instructions for their subsequent terminal effector differentiation.

Graphical Abstract

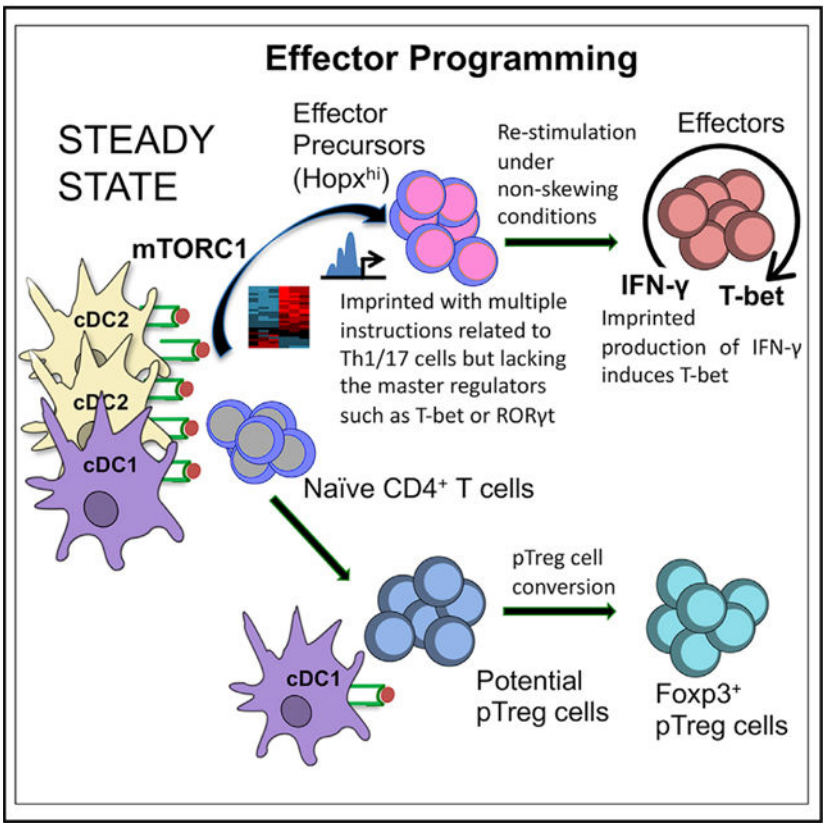

INTRODUCTION

The steady-state conditions have been considered as synonymous with an induction and maintenance of immune tolerance (Iberg and Hawiger, 2020a; Iberg et al., 2017; Steinman et al., 2003). However, T cells with effector and memory phenotype and functions can paradoxically also arise under minimal perturbations of homeostasis (Huang et al., 2003; Kawabe et al., 2017; Long et al., 2007; Vokali et al., 2020). It remains unclear how autoimmune and other effector responses can be initiated despite the presence of mechanisms that induce and maintain T cell tolerance in the steady state (ElTanbouly et al., 2020; Iberg and Hawiger, 2020a; Iberg et al., 2017; Vokali et al., 2020). The current model postulates that in the steady state, dendritic cells (DCs) with tolerogenic functions induce peripheral Foxp3^{+} regulatory T (pTreg) cells, whereas pro-inflammatory conditions skew toward priming of effector T cells (effectors) (Iberg et al., 2017; Iwasaki and Medzhitov, 2015; Merad et al., 2013; Pulendran, 2015; Segura and Amigorena, 2013; Steinman, 2012;

Yatim et al., 2017; Zelenay and Reis e Sousa, 2013). Nevertheless, after activation in the steady state, substantial numbers of the initially activated antigen-specific $CD4^+$ T cells, including among the monoclonal populations of T cell receptor transgenic (TCR tg) cells, fail to convert into pTreg cells (Iberg et al., 2017; Jones and Hawiger, 2017). Such $Foxp3^{neg}$ T cells do not induce the expression of the established key regulators of T cell fate, and the functional polarization of these T cells remains unclear (Iberg et al., 2017; Jones et al., 2016). We now found that after their antigenic activation in the steady state, $CD4^+$ T cells undergo a two-step process of fate determination that begins with an early induction of effector precursors followed by their programmed terminal differentiation. This initial process is independent of an expression of well-established master regulators of T cell fate. Instead, the effector precursors are characterized by the early induced expression of Homeodomain only protein (Hopx).

Expression of Hopx in naive $CD4^+$ T cells can be induced *de novo* during differentiation, such as during a conversion of pTreg cells (Hawiger et al., 2010; Jones et al., 2015). Hopx does not govern the initial conversion of pTreg cells, but instead Hopx controls the maintenance of mature $Foxp3^+$ pTreg cells during their suppressor functions under the pro-inflammatory conditions (Hawiger et al., 2010; Jones and Hawiger, 2017; Jones et al., 2015). Hopx is also expressed in some $Foxp3^{neg}$ differentiated lymphocytes, including $CD4^+$ effector T cells (such as cytotoxic $CD4^+$ cells) (Albrecht et al., 2010; Cano-Gamez et al., 2020; De Simone et al., 2019; Serroukh et al., 2018). In addition to lymphocytes, Hopx is also present in various non-hematopoietic tissues and organs, including brain, heart, intestines, stem cells, and various tumors (Mariotto et al., 2016). Contrasting with such semi-ubiquitous expression of Hopx, its genetic deletion leads to only a few specific abnormalities (Jones and Hawiger, 2017; Mariotto et al., 2016). Instead, Hopx has recently emerged as a crucial marker of the specific developmental/differentiation potentials of progenitor populations in various non-hematopoietic tissues both in human and mouse systems (Mariotto et al., 2016). Our current results now uncovered the key roles of Hopx in indicating specific differentiation potentials induced early in $CD4^+$ T cells following their activation in the steady state. We found that $Hopx^{hi}$ effector precursors become imprinted with transcriptional and epigenetic (defined by methylation and acetylation of the histone H3 associated with active genes and enhancers) instructions for their subsequent terminal differentiation that may result in autoimmune functions. These molecular circuits that advance such robust terminal differentiation even under minimally skewing conditions include a programmed expression of interferon-γ (IFN-γ), whose production then promotes expression of the crucial master regulator T-bet in effector precursors. Our findings further reveal that effector programming coincides with a process of regulatory conversion among T cells sharing the same antigen specificity, consistent with the maintenance of tolerance. Functions of mammalian target of rapamycin (mTOR) complex 1 (mTORC1) and antigenic activation by conventional type 2 DCs (cDC2) increase the induction of effector precursors while correspondingly reducing numbers of T cells that can become pTreg cells. Overall, a two-step process of fate determination extends the plasticity of the responses that are initiated in the immune system in the steady state.

RESULTS

Induction of Regulatory and Effector-Related T Cells in the Steady State

To examine T cells that fail to efficiently convert into Foxp3^{+} pTreg cells, we delivered a self-antigen, myelin oligodendrocyte glycoprotein (MOG), to induce a specific pTreg cell conversion by tolerogenic DEC-205^{+} DCs, using well-established methods of targeted antigen delivery *in vivo* with recombinant chimeric antibodies (Hawiger et al., 2001; Iberg and Hawiger, 2019, 2020b). Because Foxp3^{+} pTreg cells express Hopx (Hawiger et al., 2010), we used *Hopx*^{GFP}*Foxp3*^{RFP} double reporter mice (Jones et al., 2015) for this analysis. The results revealed that some T cells that remained Foxp3^{neg} also expressed Hopx (Figure S1A). We further found that expression of Hopx was induced early (before Foxp3 expression) following activation *in vivo* in about half of the T cells (Figure S1B). We also found a similar early induction of Hopx expression in other antigen-specific T cells, as well as T cells activated by their corresponding cognate antigens that were specifically delivered to DCs by targeting through either DEC-205 or CD11c present on DCs (Figures S1C and S1D). Such Foxp3^{neg} T cells with either “high” (induced) or “low” (not induced) expression of Hopx (hereafter referred to as Hopx^{hi} and Hopx^{lo} T cells) showed comparable patterns of proliferation, and also expression of multiple markers (Figure S1E), including Ly6c and CD5 that were previously identified to indicate specific differentiation potentials in T cells (Fulton et al., 2015; Henderson et al., 2015; Mandl et al., 2013; Martin et al., 2013; Persaud et al., 2014).

Because expression of Hopx was previously found in multiple various types of differentiated T cells, including Treg cells and effectors (Albrecht et al., 2010; De Simone et al., 2019; Hawiger et al., 2010; Jones et al., 2015), we hypothesized that an early induction of Hopx expression in naive T cells activated in the steady state may uniquely distinguish varying differentiation potentials of such T cells. To test this, we isolated Hopx^{hi} and Hopx^{lo} T cells that we initially induced *in vivo* and transferred these Foxp3^{neg} T cells into new recipients. We then re-stimulated such T cells with the same antigen presented *in vivo* by DEC-205^{+} DCs (Figure 1A). These conditions have been established before to promote a robust conversion of antigen-specific naive T cells into Foxp3^{+}CD25^{+} pTreg cells (Iberg et al., 2017; Jones et al., 2016), and consistently, we observed an almost 60% conversion of pTreg cells among Hopx^{lo} T cells. In contrast, significantly fewer (20%) Hopx^{hi} T cells converted into pTreg cells (Figure 1B). To independently confirm such varying Treg cell differentiation potentials of Hopx^{hi} and Hopx^{lo} T cells, we tested Hopx^{hi} and Hopx^{lo} T cells for their ability to convert into Foxp3^{+}CD25^{+} induced Treg (iTreg) cells *in vitro*. Given that most Hopx^{hi} and Hopx^{lo} T cells did not downregulate CD62L expression following their initial induction *in vivo*, we used for these and all other subsequent experiments T cells that were CD62L^{hi} (as shown in Figure S1F) to avoid skewing of the results by T cells that might have already differentiated. Such Hopx^{hi} and Hopx^{lo} (CD62L^{hi}) T cells had a similar expression of antigen-specific TCR alpha and beta chains and were also similarly activated in comparison with naive T cells as indicated by increased expression of CD69 and Nur77, as well as a downregulation of VISTA, whose expression is associated with T cell quiescence (ElTanbouly et al., 2020) (Figures S1G–S1I). However, the conversion to iTreg cells was impaired among multiple tested populations of Hopx^{hi} T cells that were specifically induced

in vivo (Figures S1J–S1L), despite a comparable survival of the Hopx^{hi}, Hopx^{lo}, and naive T cells (Figure S1M). In mature Foxp3^{+} pTreg cells, Hopx controls the maintenance of these T cells during their suppressor functions under pro-inflammatory conditions. However, Hopx does not govern the conversion of pTreg cells (Hawiger et al., 2010; Jones and Hawiger, 2017; Jones et al., 2015). In accordance with these previous results, we observed that *Hopx* $^{+/+}$ and *Hopx*$^{-/-}$Foxp3^{neg} T cells pre-activated by cognate antigen in the steady state did not differ in their specific ability to convert into iTreg cells (Figures S1N and S1O). Overall, we conclude that despite being dispensable for the induction of Treg cells, an early induction of Hopx expression in T cells activated in the steady state serves as a selective marker of their decreased potential to convert into Treg cells *de novo*.

Under homeostatic steady-state conditions, endogenous T cells are constantly exposed to stimulation by agonistic peptides originating from self, as well as foreign antigens, possibly resulting in their activation and initial differentiation. To test the expression of Hopx among such polyclonal endogenous CD4^{+} T cells, we analyzed CD4^{+}Foxp3^{neg} T cells isolated from unmanipulated TCR wild-type (WT; non-TCR tg) Hopx^{GFP}Foxp3^{RFP} mice. Consistent with a previously suggested expression of Hopx in some effector CD4^{+} T cells (Albrecht et al., 2010; Cano-Gamez et al., 2020; Serroukh et al., 2018), we found Hopx^{+} cells among the CD4^{+}Foxp3^{neg}CD62L^{lo} population. However, we also detected a small population of Hopx^{+} cells among the CD4^{+}Foxp3^{neg}CD62L^{hi} endogenous T cells (Figure S2A). We propose that this Hopx^{+}CD4^{+}Foxp3^{neg}CD62L^{hi} population arises as a result of a constant activation of polyclonal T cells under homeostatic conditions, and these T cells may correspond to Hopx^{hi} T cells that we identified above. However, it is currently not possible to distinguish polyclonal Hopx^{lo} and other T cells that lack expression of Hopx. Also, the timing of activation and induction of Hopx expression in specific T cells among the polyclonal population is rather unpredictable, further constraining an in-depth analysis of these mechanisms in the polyclonal repertoire. Therefore, to explain the observed differences in the fate of Hopx^{hi} and Hopx^{lo} T cells, we performed a transcriptome analysis of Hopx^{hi}, Hopx^{lo}, and naive T cells obtained from TCR tg animals using RNA sequencing (RNA-seq). Principal-component analysis (PCA) revealed numerous differences in the transcriptomes of these T cells, and expression of multiple individual genes differed significantly between the Hopx^{hi}, Hopx^{lo}, and naive T cells (Figures S2B and S2C). However, the genes whose expression was specifically altered in either Hopx^{hi} or Hopx^{lo} T cells in comparison with naive T cells had only a small overlap with the genes in the multiple clusters and modules that were previously identified in naive and some specifically activated T cells (ElTanbouly et al., 2020) (Figure S2D). Also, the expression of multiple master regulators of T cell differentiation (Wang et al., 2015), including *Tbx21*, *Gata3*, *Rorc*, *Sfpi1*, *Bcl6*, *Irf4*, *Batf*, *Stat3*, and *Nr4a1*, represented here as biological “averages” of their corresponding expression among huge numbers of individual cells, did not differ between such Hopx^{hi} and Hopx^{lo} T cells that are characterized by distinct and non-overlapping expression of Hopx (Figure 1C).

To characterize the relevant differences in gene expression between Hopx^{hi} and Hopx^{lo} T cells, we performed gene set enrichment analysis (GSEA) (Subramanian et al., 2005) using a comprehensive group of publicly available gene sets related to functional subsets of CD4^{+} T cells (Figure S3). This analysis revealed multiple enrichments of specific gene sets

containing genes positively associated with effector differentiation (gene expression upregulated in effector $CD4^+$ T cells) among the genes whose expression was upregulated in $Hopx^{hi}$ T cells in comparison with $Hopx^{lo}$ T cells. The specific genes identified by GSEA included genes known to govern biological processes, including development, metabolism, and proliferation (Figures S4A and S4B; Table 1). All of these specific genes were also individually present in multiple other gene sets positively associated with effector/memory T cells (Figure 1D). The expression of *Il2ra* was downregulated in $Hopx^{hi}$ T cells in comparison with $Hopx^{lo}$ T cells (Figure S4B), likely consistent with the known requirement of *Il2ra* for Treg cell differentiation and functions (Fontenot et al., 2005) and the observed decreased conversion of $Hopx^{hi}$ T cells into pTreg cells. In addition to the genes identified by GSEA, a separate literature-based analysis of the genes whose expression differed between $Hopx^{hi}$ and $Hopx^{lo}$ T cells revealed in $Hopx^{hi}$ T cells several other genes specifically associated with the differentiation of effector and memory immune cells (Figure 1E; Table 1). We also performed an analysis of microRNAs (miRNAs) whose expression significantly differed between $Hopx^{hi}$ and $Hopx^{lo}$ T cells. We found an increased expression in $Hopx^{hi}$ T cells of Mir21a, Mir183, Mir31, and Mir148a, all previously proposed to either promote T helper (Th) 1/17 effector differentiation or limit Treg cell differentiation. In contrast, expressions of Mir150 and Mir26a, both positively associated with Treg cell differentiation, were decreased in $Hopx^{hi}$ T cells (Figure S4C; Table 1). Overall, we conclude that despite the initial activation under generally tolerogenic steady-state conditions, $Hopx^{hi}$ T cells resist the conversion into Treg cells and acquire a unique transcriptional signature that includes multiple genes related to Th1/17 cells, while lacking the major master regulators of effector differentiation.

Terminal Differentiation of Effector Precursors

Based on the above results, we hypothesized that $Hopx^{hi}$ T cells might be specialized precursors of effector T cells. Consistent with this hypothesis, we found that after re-stimulation under non-skewing (Th0) conditions *in vitro*, $Hopx^{hi}$ T cells robustly induced the expression of T-bet, a crucial master regulator of Th1 differentiation. This induction of T-bet expression by $Hopx^{hi}$ T cells was highly specific, with only very few $Hopx^{lo}$ or naïve T cells inducing T-bet expression under these conditions (Figure 2A). A similar induction of T-bet expression was also observed among all other tested populations of $Hopx^{hi}$ T cells that were either of different antigen specificity or were induced *in vivo* by different subsets of cDCs (Figures S5A and S5B). In contrast, no cells in the $Hopx^{hi}$, $Hopx^{lo}$, or naive T cell populations induced expression of Foxp3 under these Th0 conditions. This is further consistent with a specific effector skewing of $Hopx^{hi}$ T cells (Figure S5C).

An activation of T cells in the steady state is known to prevent subsequent immunogenic (autoimmune) activation (Iberg et al., 2017). Therefore, to clarify the impact of terminal differentiation of $Hopx^{hi}$ T cells *in vivo* on autoimmune responses, we examined the responses of self-reactive, neural antigen (MOG)-specific $Hopx^{hi}$, $Hopx^{lo}$, and naive T cells that we transferred into separate groups of $Rag1^{-/-}$ mice that we also treated with pertussis toxin (PT) (Figure 2B). Neither $Hopx^{hi}$ nor $Hopx^{lo}$ T cells induced expression of Foxp3 (Figure S5D). However, under these mild PT-induced pro-inflammatory conditions, about 30% of $Hopx^{hi}$ T cells expressed T-bet and produced IFN-γ, a crucial cytokine of Th1

effectors (Lighvani et al., 2001; Zhu, 2018). In contrast, fewer than 10% of Hopx^{lo} or naive T cells started production of IFN-γ or T-bet expression in most animals within 11–12 days (Figures 2C and 2D; Figure S5E). About 10% of the Hopx^{hi} T cells also became double expressors of T-bet and RORγt, while such T-bet^{+}RORγt^{+} cells were almost completely absent from the Hopx^{lo} and naive populations (Figure 2E; Figure S5E). The double expression of T-bet and RORγt by Hopx^{hi} T cells could be consistent with a formation of "pathogenic" Th17 cells (Awasthi et al., 2009; Hirota et al., 2011; Lee et al., 2012; Wu et al., 2020). Overall, Hopx^{hi} T cells are effector precursors prone to an enhanced terminal effector differentiation *in vivo*.

To elucidate the relevant immune functions of the self-reactive Hopx^{hi} effector precursors, we followed the development of experimental autoimmune encephalomyelitis (EAE) in *Rag1*$^{-/-}$mice transferred with either Hopx^{hi}, Hopx^{lo}, or naive T cells and also treated with PT. This experimental system precludes any activation of other encephalitogenic T cells, therefore allowing for a direct assessment of the impact on a disease process of the effector programming of transferred T cells. Mice that received Hopx^{lo} or naive T cells developed only a baseline disease consistent with a limited induction of effectors from these T cells. In contrast, and in accordance with the robust terminal effector differentiation of Hopx^{hi} cells, mice that received these cells developed more severe symptoms of EAE (Figure 2F). Overall, we conclude that Hopx^{hi} effector precursors readily complete their terminal effector differentiation both *in vitro* and *in vivo*, and the self-reactive effector precursors can acquire enhanced autoimmune functions.

Molecular Instructions Governing the Differentiation of Effector Precursors

Because the specific transcriptional signature of effector precursors lacks master regulators known to directly govern effector differentiation, we hypothesized that the genes encoding such relevant regulators of T cell fate would be marked epigenetically for expression. To identify such epigenetic modifications associated with transcriptional activation in Hopx^{hi}, Hopx^{lo}, and naive T cells, we performed chromatin immunoprecipitation followed by sequencing (ChIP-seq) and examined trimethylation of the lysine 4 of the histone H3 (H3K4me3), as well as acetylation of the lysine 27 of the histone H3 (H3K27Ac), which are typically associated with active genes and enhancers. This analysis revealed in Hopx^{hi} effector precursors specific H3K4me3 and H3K27Ac enrichments at multiple genes, including *Ahr*, *Bhlhe40*, *Ccr6*, *Cxcr3*, *Cxcr5*, *Ifng*, *Map3k8*, *Ptger2*, and *Shcbp1* (Figure 3A). These genes encode crucial cytokines, receptors, transcription factors, and other mediators important for Th1 and Th17 effector mechanisms (Table 1), consistent with the subsequent terminal differentiation of effector precursors. However, we found no specific H3K4me3 or H3K27Ac enrichments in Hopx^{hi} effector precursors at *Tbx21* and *Rorc* genes that encode crucial master regulators T-bet and RORγt, respectively. We also found either increased or similar H3K4me3 and H3K27Ac enrichments at multiple genes in the Hopx^{lo} T cells relative to the Hopx^{hi} T cells (Figure 3B). Most such genes have no known specific functions in governing T cell differentiation. Therefore, these data stress that epigenetic programming in Hopx^{hi} T cells is overall specific to the genes relevant for T cell differentiation, and especially effector functions.

Although the genes identified above are marked by epigenetic alterations associated with transcriptional activation, most of these genes are not yet expressed in the Hopx^{hi} effector precursors (Figure 1; Figure S4). This suggests these cells may be poised for a process of terminal differentiation, dependent upon the rapidly upregulated expression of the crucial genes following T cell re-stimulation. To identify such genes, we examined by RNA-seq the transcriptomes of the Hopx^{hi}, Hopx^{lo}, and naive T cells that were re-stimulated under non-skewing conditions *in vitro*. As already shown in Figure 2A, only Hopx^{hi}, but not Hopx^{lo} or naive T, cells induce expression of T-bet under these conditions. In addition to induction of gene expression of *Tbx21* that encodes T-bet, we found in Hopx^{hi} T cells specifically increased expression of several other genes relevant for effector functions (Figure 4A; Table 1), and some of these genes were also identified in Figure 3 as epigenetically marked for expression. Among all such T cell-relevant genes whose expression in Hopx^{hi} and Hopx^{lo} T cells was found to be significantly different after the re-stimulation, but not in the absence of re-stimulation, expression of *Ifng* that encodes IFN-γ was most upregulated (Figure 4A). This rapid induction of *Ifng* expression in Hopx^{hi} T cells is consistent with the specific epigenetic modifications identified in Figure 3 in the established *Ifng* enhancer region (Shnyreva et al., 2004) and also in the promoter of *Ifngas1*, which is involved in positive regulation of *Ifng* expression (Collier et al., 2012; Gomez et al., 2013; Petermann et al., 2019). Such induced *Ifng* expression also corresponds with the robust induction of IFN-γ production observed in Hopx^{hi} T cells *in vivo* (Figure 2C), and the specific production of IFN-γ by these cells was maintained even under Treg-skewing conditions *in vitro* (Figure 4B).

IFN-γ can induce expression of T-bet (Lighvani et al., 2001; Schulz et al., 2009). We therefore hypothesized that either autocrine or paracrine production of IFN-γ by Hopx^{hi} T cells is responsible for the subsequent induction of T-bet expression in these cells. In agreement with this hypothesis, we found that blocking of IFN-γ by a specific neutralizing antibody almost completely inhibited the expression of T-bet in Hopx^{hi} T cells after their re-stimulation (Figure 4C). Collectively, these results show that the terminal differentiation of effector precursors depends on specific instructions, such as those promoting production of IFN-γ that subsequently induces expression of T-bet.

Regulation of Effector Precursor Induction

Crucial immunomodulatory pathways, such as B and T lymphocyte associated (BTLA) or programmed death-ligand 1 (PD-L1), can promote induction of pTreg cells (Francisco et al., 2009; Jones et al., 2016; Wang et al., 2008). Because we found that effector pre-determination of Hopx^{hi} T cells is accompanied by the formation of Hopx^{lo} T cells that can subsequently differentiate into pTreg cells (Figure 1), we hypothesized that specific immunomodulatory pathways may also reciprocally regulate formation of effector precursors. In agreement with the role of BTLA in promoting the conversion of Foxp3^{+} pTreg cells as we previously established (Jones et al., 2016), the percentage of developing Foxp3^{+} pTreg cells appears to be lower in the *Btla*$^{-/-}$recipients. However, neither genetic ablation of BTLA nor antibody blocking of PD-L1 affected the formation of Hopx^{hi} (Foxp3^{neg}) and Hopx^{lo} T cells (Figures S6A and S6B).

A *de novo* induction of pTreg cells is adversely affected by the activation of the mTOR (Haxhinasto et al., 2008; Sauer et al., 2008). Furthermore, mTORC1 dependent on Raptor can promote T cell priming and effector differentiation (Delgoffe et al., 2009; Geltink et al., 2018; Yang et al., 2013; Zeng and Chi, 2017). We found that despite a similar initial activation by tolerogenic DCs of *Rptor*$^{fl/fl}$ CD4^{cre} (*Rptor*$^{-/-}$) and *Rptor*$^{+/+}$ T cells, an early conversion of pTreg cells from the adoptively transferred *Rptor*$^{-/-}$T cells was increased (Figures S6C and S6D). However, mTOR has been proposed not to directly suppress Foxp3 expression in differentiating Treg cells (Harada et al., 2010; Ouyang et al., 2010). Therefore, we hypothesized that mTORC1 may instead skew the balance governing the formation of effector precursors and potential pTreg cells. In agreement with this hypothesis, we found an about 3-fold specific decrease in Hopx^{hi} effector precursor induction *in vivo* from *Rptor* $^{-/-}$Hopx^{neg}Foxp3^{neg} T cells (Figure 5A) but similar total numbers of the remaining *Rptor* $^{-/-}$and *Rptor*$^{+/+}$ T cells (Figure S6E). The small numbers of Hopx^{hi} T cells that did develop in the absence of mTORC1 could still readily induce T-bet expression upon re-stimulation under Th0 conditions, whereas, as expected, both *Rptor*$^{-/-}$and *Rptor*$^{+/+}$ Hopx^{lo} T cells failed to induce expression of T-bet (Figure 5B). Therefore, functions of mTORC1 increase the induction of effector precursors while correspondingly reducing numbers of T cells that can potentially become pTreg cells, independently of the process of subsequent terminal effector differentiation of such T cells.

Two major subsets of cDC, cDC1 and cDC2, are well established in eliciting diverse immune responses. Whereas cDC1 can efficiently uptake and present self-antigens important for induction of pTreg cells and tolerance in the steady state, cDC2 are generally poor inducers of pTreg cells (Iberg and Hawiger, 2020a; Iberg et al., 2017). In contrast, antigen presentation by cDC2 can lead to priming of multiple types of effector T cells, especially under pro-inflammatory conditions, but the roles of cDC2 in the steady state remain incompletely understood (Durai and Murphy, 2016). To examine T cell responses elicited by the antigenic stimulation specifically mediated by cDC2, we used a well-established experimental system based on chimeric antibodies specific for DCIR2 present on cDC2 to deliver antigens to these cDCs (Dudziak et al., 2007) in addition to targeting antigens through DEC-205 present on cDC1. We observed about a 50% increase in the formation of Hopx^{hi} effector precursors among T cells following their responses to the antigen presented specifically by cDC2 compared with the induction of effector precursors mediated by cDC1 (Figure 5C). Such effector precursors induced expression of T-bet that was dependent on the produced IFN-γ (Figure 5D; Figure S6F). Overall, we conclude that cDC2 mediate the induction of effector precursors more robustly than cDC1.

DISCUSSION

The current framework underlying the functions of the immune system postulates that pro-inflammatory signals induce immunity, whereas homeostatic conditions facilitate tolerance (Iberg et al., 2017; Iwasaki and Medzhitov, 2015; Merad et al., 2013; Pulendran, 2015; Segura and Amigorena, 2013; Steinman, 2012; Yatim et al., 2017; Zelenay and Reis e Sousa, 2013). Previous results also revealed a greater extent of plasticity of T cell differentiation under nominally pro-inflammatory conditions, such as the presence of commensal microorganisms, manifested through mechanisms responsible for the induction of pTreg

cells and tolerance to prevent excessive immune responses (Coombes et al., 2007; Esterházy et al., 2019; Manicassamy et al., 2010; Naik et al., 2012; Sun et al., 2007). In contrast, specific mechanisms of tolerance are induced in both $CD4^+$ and $CD8^+$ T cells following activation of these cells in the steady state as reviewed in Iberg and Hawiger (2020a), Iberg et al. (2017), and Steinman et al. (2003). However, a formation of T cells with transient effector characteristics has also been observed under the steady-state conditions, but the specific mechanisms governing the formation of effector T cells with potentially autoimmune functions have remained unclear (Huang et al., 2003; Kawabe et al., 2017; Long et al., 2007; Vokali et al., 2020).

Our results now revealed that effector programming is an integral part of fate determination induced in the steady state. Effector precursors are distinguished by a specific epigenetic and transcriptional profile that includes instructions for a subsequent terminal differentiation and acquisition of effector and autoimmune functions under minimal perturbations of homeostasis. Consistent with the maintenance of tolerance, effector programming can coincide with regulatory conversion among T cells sharing the same antigen specificity. However, our results suggest that these processes are mechanistically separate. The transcriptional profile of effector precursors lacks expression of established master regulators, such as T-bet or RORγt, but instead includes an induced expression of Hopx. Hopx expression has been found before in $Foxp3^+$ and some $Foxp3^{neg}$ lymphocytes, including $CD4^+$ effector T cells, although the absence of Hopx leads to only a few specific abnormalities (Albrecht et al., 2010; Cano-Gamez et al., 2020; De Simone et al., 2019; Hawiger et al., 2010; Jones et al., 2015; Mariotto et al., 2016; Serroukh et al., 2018). In mature $Foxp3^+$ pTreg cells, Hopx controls the maintenance of these T cells during their suppressor functions under pro-inflammatory conditions. However, Hopx does not govern the conversion of pTreg cells (Hawiger et al., 2010; Jones and Hawiger, 2017; Jones et al., 2015). An early induction of Hopx expression has recently also emerged as a specific marker of the developmental and differentiation potentials of multiple non-hematopoietic progenitor populations in brain, heart, intestines, and skin (as reviewed in Mariotto et al., 2016). Our results now uncovered that expression of Hopx crucially indicates the specifically altered differentiation potentials in $CD4^+$ T cells.

A pre-activation of $CD4^+$ and $CD8^+$ T cells was proposed before to facilitate their differentiation by acquisition of early expression of CD5 and other molecules (De Simone et al., 2019; Fulton et al., 2015; Henderson et al., 2015; Mandl et al., 2013; Persaud et al., 2014; Sood et al., 2019). $CD4^+$ $Hopx^{hi}$ effector precursors appear to be induced independently of the specific expression of established regulators of T cell responses and instead they express multiple other genes related to Th1 and Th17 cells. The molecular circuits governing the key transition of precursors into effectors include the programmed expression of specific factors encoded by genes such as *Ifng* that are rapidly induced upon re-stimulation, even under non-skewing or tolerizing conditions. The production of IFN-γ then induces expression of T-bet, a crucial master regulator of T cell differentiation. Under minimally skewing conditions, the majority of $Hopx^{hi}$ effector precursors predominantly skew toward Th1 phenotype. However, such effectors can also become $T\text{-}bet^+ROR\gamma t^+$ cells *in vivo*, and $Hopx^{hi}$ effector precursors also induce expression of genes specific for other types of Th cells, such as *Il13*. This may indicate a broader differentiation plasticity of the

effector precursors, possibly in the presence of additional signals. Overall, effector programming appears to be an integral part of fate determination induced by antigenic activation in the steady state. However, it also coincides with a regulatory conversion among T cells sharing the same antigen specificity, consistent with the maintenance of tolerance. Although tolerance is generally maintained by multiple mechanisms, including thymically derived tTreg cells (Josefowicz et al., 2012), specific mechanisms controlling the relative proportions of antigen-specific effector precursors and pTreg cells would be crucial for regulation of tolerance.

Antigen presentation by DCs is critical for T cell responses against foreign antigens, as well as self-antigens, and the decisions that determine specific T cell fates are at least in part influenced by the type of DCs that mediate T cell activation (Baptista et al., 2019; Durai and Murphy, 2016; Eisenbarth, 2019; Esterházy et al., 2019; Iberg and Hawiger, 2020a; Iberg et al., 2017). cDCs are the major population among both human and murine DCs and can be further divided into the cDC1 and cDC2 subsets based on their development and expression of specific markers (Collin and Bigley, 2018; Durai and Murphy, 2016; Guilliams et al., 2016). Although designations of cDC subsets do not strictly overlap with their distinct immune functions, the specific subsets are characterized by a degree of functional specialization, attributed to various factors, including different localization within the local architecture of immune organs, differences in the efficiencies of processing and presentation of antigens to T cells, and the presence of various immunomodulatory mechanisms (Baptista et al., 2019; Dudziak et al., 2007; Eisenbarth, 2019; Esterházy et al., 2019; Iberg et al., 2017). The recently characterized BTLA-HVEM-CD5 axis initiated by BTLA expressed in cDC1 helps to govern tolerogenic outcomes of interactions between cDCs and T cells (Bourque and Hawiger, 2019; Henderson et al., 2015; Jones et al., 2016). The BTLA signals that are mediated through HVEM in naive $CD4^+$ T cells increase expression of CD5 that promotes efficient conversion of pTreg cells in concert with other immunomodulatory mechanisms (Bourque and Hawiger, 2018; Henderson et al., 2015; Iberg and Hawiger, 2020a; Jones et al., 2016). However, we found that immunomodulatory pathways, such as those mediated by BTLA or PD-L1, do not affect the induction of $Hopx^{hi}$ T cells. Therefore, such immunomodulatory pathways might rather govern the separate process of subsequent conversion of pTreg cells from $Hopx^{lo}$ T cells.

In contrast, induction of $Hopx^{hi}$ effector precursors is enhanced by antigenic stimulation mediated specifically by cDC2. This is consistent with the robust priming of effector T cells mediated by cDC2 (Baptista et al., 2019; Dudziak et al., 2007; Durai and Murphy, 2016; Eisenbarth, 2019). Our results now clarify the roles of cDC2 in the steady state and reveal that under such conditions, cDC2 do not prime effector T cells directly but instead induce effector precursors more efficiently than cDC1. The subsequent transition of $Hopx^{hi}$ effector precursors into effectors occurs during an additional re-stimulation even under minimally skewing conditions. This is in contrast with a pTreg cell conversion process that requires the continuous presence of specific signals that can be provided by tolerogenic DCs. $Hopx^{hi}$ effector precursors resist such Treg cell-promoting signals, in accord with their effector skewing under Th0 conditions. In contrast, and consistent with their programmed expression of IL-12 receptor, under various subsequent immune conditions these cells may possibly remain susceptible to the specific signals such as IL-12, in agreement with the roles of IL-12

to control effector T cell differentiation (van Panhuys et al., 2014). Overall, various fate-modifying signals might further enable specific differentiation programs of the effector precursors.

The functions of mTOR help to sense activation of T cells, and such mechanisms were previously proposed to inhibit Treg cell induction and promote effector differentiation (Delgoffe et al., 2009; Delgoffe and Powell, 2015; Geltink et al., 2018; Haxhinasto et al., 2008; Huang and Perl, 2018; O'Sullivan and Pearce, 2015; Sauer et al., 2008; Zeng and Chi, 2017). These previous results are therefore consistent with our current findings that the functions of mTORC1 promote effector programming. However, our results now reveal that although such roles of mTORC1 promote the induction of $Hopx^{hi}$ effector precursors, mTORC1 is not essential for a terminal differentiation of these precursors. Therefore, by elucidating a two-step process of fate determination, our findings also help to clarify crucial roles of mTORC1 in governing priming of effectors under conditions that are relevant for autoimmune and possibly some other immune responses. Further, by dissociating the processes of the initial T cell fate commitment and subsequent terminal differentiation, our current findings also resolve an outstanding issue of how mTORC1 maintains the balance between the effector and regulatory T cell differentiation. Previous observations suggested an inhibition of Foxp3 expression by mTOR, but the corresponding mechanisms have remained unclear because other results disconnected the direct functions of mTOR and an inhibition of Foxp3 expression in T cells (Harada et al., 2010; Ouyang et al., 2010). By elucidating that mTORC1 specifically reduces the number of T cells that can potentially convert into pTreg cells, our results now explain how mTORC1 limits pTreg cell conversion without directly inhibiting Foxp3 expression in T cells. Future investigation may further clarify the detailed molecular mechanisms of mTORC1 relevant for these processes.

Overall, our results help to clarify the functions of cDCs initiating effector priming under minimal perturbations of homeostasis. We propose that current findings are in agreement with the emerging concepts of "homeostatic maturation" of cDCs and also build on the roles of DCs originally envisioned by Ralph Steinman to function as "Nature's adjuvant" inherently able to initiate certain immune and, particularly, autoimmune responses (Ardouin et al., 2016; Baratin et al., 2015; Jiang et al., 2007; Steinman, 1996, 2007; Vander Lugt et al., 2017). However, the capacity of such cDCs to initiate effector T cell differentiation in the steady state has remained unclear in light of the seminal functions of the pathways triggered by pro-inflammatory signals that crucially promote effector responses (Iwasaki and Medzhitov, 2015; Merad et al., 2013; Pulendran, 2015; Sancho and Reis e Sousa, 2012; Segura and Amigorena, 2013; Yatim et al., 2017; Zelenay and Reis e Sousa, 2013). Based on our current findings, we propose that the effector programming in the steady state can trigger certain immune responses, including those directed against self, that may possibly be then further advanced by the pro-immunogenic mechanisms mediated by the recognition of specific molecular patterns and other signals. We also would like to speculate that in accord with the key roles of $CD4^+$ T cells to promote $CD8^+$ T cell responses during immunosurveillance (Alspach et al., 2019; Ferris et al., 2020), the programming of effectors under minimal perturbations of homeostasis might help to initiate T cell responses against tumors. Eventually, the regulation of the two-step process of effector programming and

differentiation might be harnessed for future immunotherapies skewing the balance between immunity and tolerance.

STAR★METHODS

RESOURCE AVAILABILITY

Lead contact—Further information and requests for resources and reagents should be directed to and will be fulfilled by the Daniel Hawiger (daniel.hawiger@health.slu.edu).

Materials availability—This study did not generate new unique reagents.

Data and code availability—The accession numbers for the RNA-seq and ChIP-seq data reported in this paper are GEO: GSE120277, GSE141724.

EXPERIMENTAL MODEL AND SUBJECT DETAILS

Mice—All mouse strains were bred on C57BL/6 background for at least 12 generations. 6–9 week old sex- and age-matched male or female littermates were used for experiments. Littermates of the same sex were randomly assigned to experimental groups. 2D2 TCR tg mice (Bettelli et al., 2003) or OTII TCR tg (Barnden et al., 1998) were crossed onto *Hopx*$^{-/-}$ (Shin et al., 2002) or *Hopx*^{GFP} (Takeda et al., 2013) and *Foxp3*^{RFP} (Wan and Flavell, 2005) reporter mice to derive 2D2 *Hopx*$^{-/-}$ *Foxp3*^{RFP}, 2D2 *Hopx*^{GFP} *Foxp3*^{RFP} or OTII *Hopx*^{GFP} *Foxp3*^{RFP} mice respectively. Additionally, mice were crossed with *Rptor*$^{fl/fl}$ (Peterson et al., 2011) and CD4-cre (Lee et al., 2001) mice to generate 2D2 *Rptor*$^{fl/fl}$ CD4-cre *Hopx*^{GFP} *Foxp3*^{RFP} mice. TCR tg were maintained by crossing with non-carriers within the individual specific genotypes. *Btla*$^{-/-}$ (Sedy et al., 2005), *Rag1*$^{-/-}$ (Mombaerts et al., 1992) and C57BL/6 congenically mismatched recipient mice for adoptive transfer experiments were all purchased from Jackson Laboratories. All mice were maintained in our facility under specific pathogen free conditions and used in accordance with the guidelines of the Saint Louis University Institutional Animal Care and Use Committee.

METHOD DETAILS

***In vivo* targeting of antigens to DC—**Antigen-specific T cells were activated *in vivo* by cognate antigens ($MOG_{35–55}$ or $OVA_{323–339}$) that were delivered by chimeric antibodies specific to DEC-205, CD11c, or DCIR2 (Dudziak et al., 2007; Hawiger et al., 2004, 2010; Jones et al., 2016). Antibodies were produced and mice were specifically treated with corresponding MOG or OVA delivering chimeric antibodies as previously established (Hawiger et al., 2004, 2010) and further described in (Jones et al., 2016). Briefly, antibodies were expressed in A293 cells (ATCC) by transient transfection of plasmids using calcium-phosphate. Cells were grown in serum-free DMEM supplemented with Nutridoma SP (Roche) and antibodies were purified on protein-G Sepharose beads (GE Healthcare). Chimeric antibodies were injected in PBS intraperitoneally at 12.5 μg/mouse (MOG-delivering antibodies) or 250 ng/mouse (OVA-delivering antibodies) as established previously (Hawiger et al., 2004, 2010; Jones et al., 2016).

Experimental autoimmune encephalomyelitis (EAE)—*Rag1*$^{-/-}$ recipients of 2D2 T cells were injected intraperitoneally with 200 ng per mouse of Pertussis toxin (List Biological Laboratories Inc.) reconstituted in PBS on days 1 and 3 after T cell transfer. Clinical disease score of EAE was graded on a scale of 0–4: 0 – no clinical signs; 1 – flaccid tail; 2 – hind limb weakness; abnormal gait; 3 – complete hind limb paralysis; 4 – complete hind limb paralysis and forelimb weakness or paralysis. Mice were scored daily in a blinded fashion.

***In vitro* T cell stimulation—**Treg cell induction *in vitro* was performed by culturing 0.2 × 10^6 sorted T cells/well in 96 well plates pre-coated with anti-CD3 (145–2C11) (1 μg/mL) using Click's media (Millipore-Sigma) containing 10% fetal bovine serum (FBS) (Gemini); penicillin-streptomycin, L-glutamine, HEPES, β-mercaptoethanol, sodium pyruvate (all from GIBCO); recombinant mouse IL-2 (200 units/ml), human TGF-β1 (0.25 ng/ml, or as indicated in figure legends of individual figures), and anti-CD28 (37.51) (1.5 μg/mL) (Biolegend).

Th0 cultures were prepared by culturing 0.2 × 10^6 sorted T cells/well with 0.1 × 10^6 antigen presenting cells (APCs) in the presence of anti-CD3 (145–2C11) (1 μg/ml) (Biolegend) using Click's media (Millipore-Sigma) containing 10% FBS (Gemini) and penicillin-streptomycin, L-glutamine, β-mercaptoethanol, HEPES, and sodium pyruvate (all from GIBCO) for 1–3 days. The APCs used in these cultures were isolated from pooled lymph node and spleen cells depleted of T cells ($CD4^+$, $CD8^+$, $CD3^+$) and $CD49b^+$ NK cells using biotinylated antibodies (Biolegend) and magnetic microbead selection (Miltenyi).

Flow Cytometry—Lymphocytes from peripheral lymph nodes and spleens were isolated and analyzed separately unless otherwise indicated. Similar results were obtained from spleens and peripheral lymph nodes from corresponding experimental groups. For surface marker staining, cells were first analyzed with Zombie Aqua Live/Dead viability dye according to manufacturer's protocol (BioLegend), pre-incubated with Fc-block (anti-CD16/32, clone 2.4G2, produced in-house from corresponding hybridomas obtained from ATCC), and then stained with fluorochrome-conjugated antibodies for 25 minutes at 4°C. To conduct intracellular staining for transcription factors, cell populations as described in the manuscript were sorted then fixed and permeabilized according to manufacturer's protocol (eBioscience). Alternatively, sorted T cell populations were cultured *in vitro* as described in the manuscript and then processed as above. Additionally, *ex vivo* isolated T cells obtained as described in the manuscript from individual groups of *Rag1*$^{-/-}$ recipients were fixed and stained for transcription factors as above. To conduct intracellular staining for cytokines, *ex vivo* isolated T cells obtained as described in the manuscript from individual groups of *Rag1*$^{-/-}$ recipients were stimulated for approximately 4 hours with phorbol 12-myristate 13-acetate (PMA) (Millipore-Sigma) (100ng/ml), and Ionomycin (Millipore-Sigma) (0.25 μM). BD GolgiStop Protein Transport Inhibitor (containing monensin) was added for the last 2 hours, and cells were fixed and permeabilized with Cytofix-Cytoperm buffers according to manufacturer's protocol (BD). Flow cytometry acquisition was performed using BD LSR II or BD LSRFortessa instruments, and data was analyzed with FlowJo software (FlowJo, LLC).

Antibodies used for flow cytometry and *in vitro* culture experiments— Antibodies and reagents used for experiments include anti-CD11c (N418), anti-CD11b (M1/70), anti-CD8a (53–6.7), anti-B220 (RA3–6B2), anti-CD49B (DX5), anti-CD25 (PL61), Streptavidin (405232), anti-CD4 (GK1.5), anti-CD45.2 (104), anti-CD62L (Mel-14), Ly-6C (AL-21), anti-IFN-γ (XMG1.2), anti-CD3 (145–2C11), Rat IgG1 Isotype control (RTK2071), anti-CD28 (37.51), anti-CD5 (53–7.3), anti-VISTA (MIH63), anti-T-bet (4B10), (BioLegend), anti-CD69 (H1.2F3), anti-RORgt (q31–378), anti-TCR V beta 11 (RR3–15), anti-Nur77 (12.14), (BD), anti-TCR V alpha 3.2 (RR3–16), anti-Foxp3 (FJK-16 s), Fc-block (anti-CD16/32) (2.4G2), (ATCC).

Cytokine measurement—Cytokine concentrations were measured using a BD Cytometric Bead Array (CBA) mouse cytokine kit according to manufacturer's protocols.

IFN-γ blocking—IFN-γ was blocked *in vitro* by using 10 ug/ml of anti-IFN-γ (XMG1.2) (BioXcell) or purified Rat IgG1, k Isotype Control Antibody (RTK2071) (Biolegend).

T cell isolation and sorting—Lymph nodes and spleens were pooled, and $CD4^+$ T cells were enriched by depletion. Non-CD4 T cells were stained with anti-CD8a (53–6.7), B220 (RA3–6B2), CD11c (N418), CD11b (M1/70), and CD49b(DX5) biotinylated antibodies (Biolegend) followed by magnetic microbead selection (Miltenyi). Cells were sorted on FACSAria III or FACSAria Fusion instruments (BD). Th0 cultures were harvested after 12 hours and stained with fluorochrome-conjugated anti-CD4 and Zobmie Auqua Live/Dead viability dye and sorted as described above.

***In vivo* cell proliferation assay—**T cell proliferation *in vivo* was assessed by using eBioscience™ Cell Proliferation Dye eFluor™ 450 according to manufacturer's protocol. Briefly, sorted T cells were washed in PBS and stained in 10 μM dye in PBS at concentration 10×10^7 cells/mL at room temperature for 20 minutes. Next, the staining was quenched by adding FBS, and the cells were washed and transferred to recipient animals.

T cell adoptive transfers—Sorted cells were washed twice with PBS and counted. Cells were then reconstituted in PBS and injected into tail veins. 5×10^6 T cells were transferred into C57BL/6 recipients, and 3×10^6 T cells were transferred into *Rag1*$^{-/-}$ recipients.

PD-L1 blocking—αPD-L1 (10F.9G2) (150 μg/mouse) antibody (BioXCell) was injected in PBS i.p. 4 and 26 hours after chimeric antibodies were administered

RNA library construction and sequencing—Total mRNA and miRNA were isolated by using TRIzol reagent (Invitrogen) and mirVana miRNA isolation Kit (Invitrogen) to isolate both large and small RNA from $Hopx^{hi}$, $Hopx^{lo}$, and naive 2D2 $CD4^+$ T cells obtained as described in (Figure S1F). In some experiments individual T cell groups were additionally re-stimulated *in vitro* and $CD4^+$ T cells were then re-sorted. The material for every replicate within each of the $Hopx^{hi}$, $Hopx^{lo}$, and naive T cell groups was obtained from an independent experiment. Within each such an independent experiment $Hopx^{hi}$ and $Hopx^{lo}$ T cells were pooled from multiple (5–6) mice 5 days after treatment with αDEC-MOG; the naive T cells were pooled from multiple (4–5) mice that were treated with PBS.

Ribosomal RNA was depleted from total RNA using the Eukaryotic RiboMinus Core Module v2 (Life Technologies, ThermoFisher), and libraries were constructed using the Ion Total RNA-seq v2 kit (Life Technologies, ThermoFisher) according to the manufacturer's protocol. Sequencing was performed on an Ion Torrent Proton with a mean read length of ~140 nucleotides, and reads were aligned to the mm10 mouse genome assembly using the TMAP (Torrent Mapping Program) aligner (Homer, 2011) map4 algorithm. Reads required a minimum seed length of 20 nucleotides, and soft-clipping at both 5′ and 3′ ends was permitted to accommodate spliced reads. Analysis methods that count reads operate under the assumption that reads in each sample are of the same length. Unlike some other platforms (for example Illumina), Ion Torrent Proton platform generates reads which are variable in length. To help ensure that differences in read lengths do not impact the quantification of the expression of each gene, the number of nucleotides within each read that aligns to gene's exons were counted using the *genomecoveragebed* program included in the freely available BEDtools (Quinlan and Hall, 2010). As most recently described in (Basta et al., 2020; Kreienkamp et al., 2018), total exon coverage was calculated for each sample and divided by the average total exon coverage across all replicates to obtain normalization factors. The summed coverage for each gene in each replicate was then multiplied by these normalization factors to obtain expression values for each gene as total normalized nucleotide coverage.

Small RNA-seq libraries were constructed using the Ion Total RNA-seq v2 kit (Life Technologies, Thermofisher) according to the manufacturer's protocol for small RNA libraries. Sequencing was performed on an Ion Torrent Proton with a mean read length of ~55 nucleotides, and reads were aligned to the *Mus musculus* (house mouse) genome assembly GRCm38 (mm10) from Genome Reference Consortium using the TMAP aligner (Homer, 2011) as described above. The nucleotide coverage for miRNAs was calculated and normalized to total coverage as above. Expression values are given as total normalized nucleotide coverage per miRNA.

Analysis of gene expression—Expression values were identified for 23219 genes in three individual replicates for each experimental group ($Hopx^{hi}$, $Hopx^{lo}$, and naive T cells). Within each group, the mean expression values were calculated for every gene that had at least one replicate with the expression value above 5. Expression values below 5 were considered as "undetected" and excluded from averaging. If all three replicates were undetected, then the mean expression value of that gene within the given group was set as equal to 1. The genes specifically expressed (expression values greater than 10^3 in all replicates) in both groups within each comparison were analyzed by t test as described in "Quantification and statistical analysis" below. The genes whose mean expression values differed between two compared groups by at least 2-fold and that were either specifically expressed in both groups within each comparison with a p value less than 0.05 or that were classified as specifically expressed in one group, but not in the other group within each comparison were then used for subsequent Gene Set Enrichment Analysis (GSEA) as well as for additional literature-based analysis. As required for GSEA analysis, the official mouse gene symbols were converted first to the ENSEMBL format and then to HUGO format using the BioMart tool (http://useast.ensembl.org/biomart/martview/

c0a53d4785d930f83bf91ca0b07f7f18) in conjunction with the ENSEMBL_mouse_gene.chip dictionary available in the GSEA web page. In rare cases when a gene was absent in these dictionaries, its official mouse gene symbol was converted to uppercase and used directly as a HUGO format unless multiple alternative translation variants were present. After the name conversion, 1525 genes were pooled in the comparison between $Hopx^{hi}$ and naive T cells, 813 genes were pooled in the comparison between $Hopx^{lo}$ and naive T cells, and 372 genes were pooled in the comparison between $Hopx^{hi}$ and $Hopx^{lo}$ T cells. Each of those three gene lists was submitted independently to GSEA Preranked with the following metric:

$$\log_2 \frac{\text{mean expression in the first group}}{\text{mean expression in the second group}}$$

GSEA were performed using a customized database of published gene sets containing the genes against which we tested. This specific database was constructed from the c7.all.v6.1 database (https://www.gsea-msigdb.org/gsea/downloads.jsp) by selecting those gene sets whose titles contained at least one of the "positive" keywords (CD4, TREG, TEFF, _TH_, TFH, ROR, FOXP3, T-BET, GATA3) and none of the "negative" keywords (CD8, DN_, DP, DC, DENDRITIC, MACROPHAGE, BCELL, MAST, THYMUS, MEDULLA, CORTEX, MYELOID, KO). The resulting database contained 994 gene sets and is denoted herein as "$CD4^+$ T cell-related gene sets."

For RNA-seq analysis of T cells following their re-stimulation *in vitro*, expression values were identified for 3 replicates of each $Hopx^{hi}$ T cells, $Hopx^{lo}$ T cells, and naive T cells after excluding snoRNA exons from all samples. The expression values less than 10^(1.5) ≈31.6 were considered undetected and excluded from averaging as described above. Genes were then analyzed as described in the section above. Additionally, the analysis included genes that had expression values higher than 150 in all three replicates of $Hopx^{hi}$ T cells, but whose expression was undetected in all replicates of $Hopx^{lo}$ and naive T cells. All identified genes whose expression had not been significantly different between $Hopx^{hi}$ and $Hopx^{lo}$ T cells before the *in vitro* re-stimulation, were selected and then further analyzed based on the literature search.

Analysis of miRNA expression—Expression values were identified for 2220 miRNAs in three individual replicates for each experimental group ($Hopx^{hi}$, $Hopx^{lo}$, and naive T cells). Within each group, the mean expression values were calculated for every miRNA that had at least one replicate with the expression value above 5. Expression values below 5 were considered as "undetected" and excluded from averaging. If all three replicates were undetected, then the mean expression value of that miRNA within the given group was set as equal to 1. The miRNAs specifically expressed (expression values greater than 200 in all replicates) were additionally tested by t test, as described in "Quantification and statistical analysis" below, followed by the positive false discovery rate correction (Storey and Tibshirani, 2003). The miRNAs whose mean expression values differed between $Hopx^{hi}$ and $Hopx^{lo}$ T cells by at least 2-fold and that were either specifically expressed in both groups with a confidence value of at least 0.05, or that were classified as specifically expressed in only one group, but not in the other group were identified. In total, 48 miRNAs were

identified and for normalization their expression values were divided by the mean expression values of the corresponding miRNAs in the naive group.

Chromatin Isolation—After sorting, cells were adjusted to 2×10^6 cells/ml in 3%–5% FCS in PBS. Cells were fixed with 1% formaldehyde for 12 minutes at room temperature. Fixation was stopped by adding glycine to a final concentration of 0.25M. Cells were collected by centrifugation at 1000 g for 5 minutes, washed twice with cold PBS, and frozen as a pellet on dry ice and stored at −80°C. Chromatin was prepared as previously described (Dorsett et al., 2014; Swain et al., 2016) with slight modifications. To isolate chromatin, 10×10^6 cells were suspended in 300 mL sonication buffer [0.4% SDS, 10mM Tris pH 7.6] with protease inhibitors (Roche cOmplete, EDTA-free Protease Inhibitor Cocktail) and incubated on ice for 20 minutes. The cell suspension was sonicated, and chromatin was sheared to a range of 200–1000bp using a Diagenode Biorupter. After sonication, 900 μL of adjustment buffer [10mM Tris pH 7.6, 1.33 mM EDTA pH 8, 0.133% Na deoxycholate, 1.33% Triton] plus protease inhibitors was added and chromatin was incubated on ice for an additional 20 minutes. Chromatin was clarified by centrifugation at 16,000 g for 10 minutes at 4°C. The supernatant was collected and glycerol was added to a final concentration of 5% prior to snap freezing on dry ice and storing at −80°C.

ChIP-seq—Multiple independent biological replicates were performed for each ChIP-seq experiment. All ChIP antibodies were purchased from Cell Signaling Technology: H3K4me3 (Rabbit mAb9751), H3K27Ac (Rabbit mAb8173). To perform ChIP, 600 mL of chromatin (~5×10^6 cells) was used. Chromatin was precleared by incubating with 15ul Protein A Dynabeads (Invitrogen) that were pre-washed with RIPA Buffer [10mM Tris pH 7.6, 1mM EDTA pH 8, 0.1% SDS, 0.1% Na deoxycholate, 1% Triton] for 2 hours at 4°C. Beads were discarded and 5ul of antibody was incubated with the chromatin overnight at 4°C. The chromatin-antibody mix was then incubated with 20ul of Protein A Dynabeads (prewashed with 0.5% BSA in PBS) at 4°C for 4 hours. Beads were washed 5 times for 5 minutes each at room temperature with cold wash buffer [50mM HEPES pH 7.5, 1mM EDTA, 1% NP-40, 0.7% Na Deoxycholate, 500mM LiCl] and 4 times with cold TE. Bound chromatin was eluted by suspending beads in 200 μL Elution Buffer [50mM Tris HCl pH 8, 10mM EDTA, 1% SDS] and incubating at 65°C for 40 minutes with mixing. After discarding the beads, 200 μL of 0.2 μg/μl RNase A (QIAGEN, 158924) in TE was added to the supernatant and incubated for 1 hour at 37°C. To reverse the crosslinks, Proteinase K (Roche, 03115828001) was added to a final concentration of 0.5mg/mL and incubated at 65°C overnight (up to 15 hours). Immunoprecipitated DNA was purified using MinElute columns (QIAGEN) and the concentration measured using a Qubit Fluorometer. A nanogram of the DNA was sheared to an average size of 150 to 200 nt by sonication and used to make ChIP-seq libraries using the Ion Plus Fragment Library Kit (Life Technologies) without enzymatic shearing.

ChIP-seq processing—ChIP-seq libraries were sequenced on an Ion Torrent Proton to approximately 2X genome coverage and input chromatin libraries were sequenced to approximately 8x genome coverage. Reads were aligned to the mm10 mouse genome assembly using the TMAP (Homer, 2011) aligner map4 algorithm without soft-clipping.

Reads flagged as PCR duplicates were removed using Samtools (Li et al., 2009). Genome coverage was calculated for ChIP and input samples using BedTools (Quinlan and Hall, 2010). ChIP sample coverage was normalized to input coverage in R (R Development Core Team, 2015) using a previously described script (Dorsett and Misulovin, 2017) to generate ChIP enrichment values every 50 bp in sgr files. Prior to averaging independent biological replicates, they were assessed for reproducibility both visually in IGB (Freese et al., 2016) and by genome-wide Pearson correlation coefficients. To allow for quantitative comparisons between groups, average enrichment values from naive, $Hopx^{hi}$ and $Hopx^{lo}$ groups for each antibody were quantile normalized to each other using the normalize.quantiles command in R, from the preprocessCore package. Quantile normalized average enrichment values were used for all downstream analysis.

QUANTIFICATION AND STATISTICAL ANALYSIS

Mice of particular genotypes were randomly assigned to individual experimental groups. All experimental groups and individual mice were included in statistical analysis. The data was collected from 2–5 independent experiments of each kind. *P* values were calculated using unpaired two-tailed t test (Welch's unequal variances t test), paired two-tailed t test (Student's t test) (for comparisons of gene expression in $Hopx^{hi}$ and $Hopx^{lo}$ groups whose corresponding replicates were both obtained from the same cohorts of mice) and two-way ANOVA. Additional specific statistical analysis and corrections are listed in respective figure legends and elsewhere in methods. Statistical analysis was performed using MATLAB (The MathWorks) and GraphPad (Prism). No new methods were used to determine whether the data met assumptions of the statistical approach.

Supplementary Material

Refer to Web version on PubMed Central for supplementary material.

ACKNOWLEDGMENTS

The authors would like to thank Joy Eslick and Sherri L. Koehm (Saint Louis University Flow Cytometry Core) for expert help with flow cytometry, and Kathy Mihindukulasuriya (Saint Louis University Genomic Core) for assistance with RNA-seq. This work was supported in part by grants from National Institute of Allergy and Infectious Diseases of the National Institutes of Health (R01AI113903 to D.H.) and National Multiple Sclerosis Society (RG-1902-33632 to D.H.).

REFERENCES

Acuff NV, Li X, Kirkland R, Nagy T, and Watford WT (2015). Tumor progression locus 2 differentially regulates IFNγ and IL-17 production by effector CD4+ T cells in a T cell transfer model of colitis. PLoS ONE 10, e0119885. [PubMed: 25781948]

Albrecht I, Niesner U, Janke M, Menning A, Loddenkemper C, Kühl AA, Lepenies I, Lexberg MH, Westendorf K, Hradilkova K, et al. (2010). Persistence of effector memory Th1 cells is regulated by Hopx. Eur. J. Immunol 40, 2993–3006. [PubMed: 21061432]

Alspach E, Lussier DM, Miceli AP, Kizhvatov I, DuPage M, Luoma AM, Meng W, Lichti CF, Esaulova E, Vomund AN, et al. (2019). MHC-II neoantigens shape tumour immunity and response to immunotherapy. Nature 574, 696–701. [PubMed: 31645760]

Ardouin L, Luche H, Chelbi R, Carpentier S, Shawket A, Montanana Sanchis F, Santa Maria C, Grenot P, Alexandre Y, Grégoire C, et al. (2016). Broad and Largely Concordant Molecular Changes

Characterize Tolerogenic and Immunogenic Dendritic Cell Maturation in Thymus and Periphery. Immunity 45, 305–318. [PubMed: 27533013]

Awasthi A, Riol-Blanco L, Jäger A, Korn T, Pot C, Galileos G, Bettelli E, Kuchroo VK, and Oukka M (2009). Cutting edge: IL-23 receptor gfp reporter mice reveal distinct populations of IL-17-producing cells. J. Immunol 182, 5904–5908. [PubMed: 19414740]

Balamurugan K, Luu VD, Kaufmann MR, Hofmann VS, Boysen G, Barth S, Bordoli MR, Stiehl DP, Moch H, Schraml P, et al. (2009). Onconeuronal cerebellar degeneration-related antigen, Cdr2, is strongly expressed in papillary renal cell carcinoma and leads to attenuated hypoxic response. Oncogene 28, 3274–3285. [PubMed: 19581925]

Baptista AP, Gola A, Huang Y, Milanez-Almeida P, Torabi-Parizi P, Urban JF Jr., Shapiro VS, Gerner MY, and Germain RN (2019). The Chemoattractant Receptor Ebi2 Drives Intranodal Naive $CD4^+$ T Cell Peripheralization to Promote Effective Adaptive Immunity. Immunity 50, 1188–1201.e6. [PubMed: 31053504]

Baratin M, Foray C, Demaria O, Habbeddine M, Pollet E, Maurizio J, Verthuy C, Davanture S, Azukizawa H, Flores-Langarica A, et al. (2015). Homeostatic NF-κB Signaling in Steady-State Migratory Dendritic Cells Regulates Immune Homeostasis and Tolerance. Immunity 42, 627–639. [PubMed: 25862089]

Barnden MJ, Allison J, Heath WR, and Carbone FR (1998). Defective TCR expression in transgenic mice constructed using cDNA-based alpha- and beta-chain genes under the control of heterologous regulatory elements. Immunol. Cell Biol 76, 34–40. [PubMed: 9553774]

Basta JM, Singh AP, Robbins L, Stout L, Pherson M, and Rauchman M (2020). The core SWI/SNF catalytic subunit Brg1 regulates nephron progenitor cell proliferation and differentiation. Dev. Biol 464, 176–187. [PubMed: 32504627]

Bettelli E, and Kuchroo VK (2005). IL-12- and IL-23-induced T helper cell subsets: birds of the same feather flock together. J. Exp. Med 201, 169–171. [PubMed: 15657286]

Bettelli E, Pagany M, Weiner HL, Linington C, Sobel RA, and Kuchroo VK (2003). Myelin oligodendrocyte glycoprotein-specific T cell receptor transgenic mice develop spontaneous autoimmune optic neuritis. J. Exp. Med 197, 1073–1081. [PubMed: 12732654]

Boniface K, Bak-Jensen KS, Li Y, Blumenschein WM, McGeachy MJ, McClanahan TK, McKenzie BS, Kastelein RA, Cua DJ, and de Waal Malefyt R (2009). Prostaglandin E2 regulates Th17 cell differentiation and function through cyclic AMP and EP2/EP4 receptor signaling. J. Exp. Med 206, 535–548. [PubMed: 19273625]

Bourque J, and Hawiger D (2018). Immunomodulatory Bonds of the Partnership between Dendritic Cells and T Cells. Crit. Rev. Immunol 38, 379–401. [PubMed: 30792568]

Bourque J, and Hawiger D (2019). The BTLA-HVEM-CD5 Immunoregulatory Axis-An Instructive Mechanism Governing pTreg Cell Differentiation. Front. Immunol 10, 1163. [PubMed: 31191536]

Buckley MW, Arandjelovic S, Trampont PC, Kim TS, Braciale TJ, and Ravichandran KS (2014). Unexpected phenotype of mice lacking Shcbp1, a protein induced during T cell proliferation. PLoS ONE 9, e105576. [PubMed: 25153088]

Caielli S, Veiga DT, Balasubramanian P, Athale S, Domic B, Murat E, Banchereau R, Xu Z, Chandra M, Chung CH, et al. (2019). A $CD4^+$ T cell population expanded in lupus blood provides B cell help through interleukin-10 and succinate. Nat. Med 25, 75–81. [PubMed: 30478422]

Cano-Gamez E, Soskic B, Roumeliotis TI, So E, Smyth DJ, Baldrighi M, Willé D, Nakic N, Esparza-Gordillo J, Larminie CGC, et al. (2020). Single-cell transcriptomics identifies an effectorness gradient shaping the response of $CD4^+$ T cells to cytokines. Nat. Commun 11, 1801. [PubMed: 32286271]

Capecchi MR, and Pozner A (2015). ASPM regulates symmetric stem cell division by tuning Cyclin E ubiquitination. Nat. Commun 6, 8763. [PubMed: 26581405]

Cayrol R, Wosik K, Berard JL, Dodelet-Devillers A, Ifergan I, Kebir H, Haqqani AS, Kreymborg K, Krug S, Moumdjian R, et al. (2008). Activated leukocyte cell adhesion molecule promotes leukocyte trafficking into the central nervous system. Nat. Immunol 9, 137–145. [PubMed: 18157132]

Chauhan AK, Moore TL, Bi Y, and Chen C (2016). FcγRIIIa-Syk Co-signal Modulates CD4+ T-cell Response and Up-regulates Toll-like Receptor (TLR) Expression. J. Biol. Chem 291, 1368–1386. [PubMed: 26582197]

Chen X, Zhu Y, Wang Z, Zhu H, Pan Q, Su S, Dong Y, Li L, Zhang H, Wu L, et al. (2016). mTORC1 alters the expression of glycolytic genes by regulating KPNA2 abundances. J. Proteomics 136, 13–24. [PubMed: 26844761]

Chiang SCC, Wood SM, Tesi B, Akar HH, Al-Herz W, Ammann S, Belen FB, Caliskan U, Kaya Z, Lehmberg K, et al. (2017). Differences in Granule Morphology yet Equally Impaired Exocytosis among Cytotoxic T Cells and NK Cells from Chediak-Higashi Syndrome Patients. Front. Immunol 8, 426. [PubMed: 28458669]

Collier SP, Collins PL, Williams CL, Boothby MR, and Aune TM (2012). Cutting edge: influence of Tmevpg1, a long intergenic noncoding RNA, on the expression of Ifng by Th1 cells. J. Immunol 189, 2084–2088. [PubMed: 22851706]

Collin M, and Bigley V (2018). Human dendritic cell subsets: an update. Immunology 154, 3–20. [PubMed: 29313948]

Coombes JL, Siddiqui KR, Arancibia-Cárcamo CV, Hall J, Sun CM, Belkaid Y, and Powrie F (2007). A functionally specialized population of mucosal CD103+ DCs induces Foxp3+ regulatory T cells via a TGF-beta and retinoic acid-dependent mechanism. J. Exp. Med 204, 1757–1764. [PubMed: 17620361]

Cui Y, Chen X, Zhang J, Sun X, Liu H, Bai L, Xu C, and Liu X (2016). Uhrf1 Controls iNKT Cell Survival and Differentiation through the Akt-mTOR Axis. Cell Rep. 15, 256–263. [PubMed: 27050515]

De Simone G, Mazza EMC, Cassotta A, Davydov AN, Kuka M, Zanon V, De Paoli F, Scamardella E, Metsger M, Roberto A, et al. (2019). CXCR3 Identifies Human Naive $CD8^+$ T Cells with Enhanced Effector Differentiation Potential. J. Immunol 203, 3179–3189. [PubMed: 31740485]

Deepak P, and Acharya A (2012). Interleukin-13 induces T helper type 2 immune responses in OVA-immunized BALB/c mice bearing a T cell lymphoma. Scand. J. Immunol 75, 85–95. [PubMed: 21923743]

Delgoffe GM, and Powell JD (2015). Feeding an army: The metabolism of T cells in activation, anergy, and exhaustion. Mol. Immunol 68 (2 Pt C), 492–496. [PubMed: 26256793]

Delgoffe GM, Kole TP, Zheng Y, Zarek PE, Matthews KL, Xiao B, Worley PF, Kozma SC, and Powell JD (2009). The mTOR kinase differentially regulates effector and regulatory T cell lineage commitment. Immunity 30, 832–844. [PubMed: 19538929]

Dhaeze T, Tremblay L, Lachance C, Peelen E, Zandee S, Grasmuck C, Bourbonnière L, Larouche S, Ayrignac X, Rébillard RM, et al. (2019). CD70 defines a subset of proinflammatory and CNS-pathogenic T_H1/T_H17 lymphocytes and is overexpressed in multiple sclerosis. Cell. Mol. Immunol 16, 652–665. [PubMed: 30635649]

Diril MK, Ratnacaram CK, Padmakumar VC, Du T, Wasser M, Coppola V, Tessarollo L, and Kaldis P (2012). Cyclin-dependent kinase 1 (Cdk1) is essential for cell division and suppression of DNA re-replication but not for liver regeneration. Proc. Natl. Acad. Sci. USA 109, 3826–3831. [PubMed: 22355113]

Dorsett D, and Misulovin Z (2017). Measuring Sister Chromatid Cohesion Protein Genome Occupancy in Drosophila melanogaster by ChIP-seq. Methods Mol. Biol 1515, 125–139. [PubMed: 27797077]

Dorsett Y, Zhou Y, Tubbs AT, Chen BR, Purman C, Lee BS, George R, Bredemeyer AL, Zhao JY, Sodergen E, et al. (2014). HCoDES reveals chromosomal DNA end structures with single-nucleotide resolution. Mol. Cell 56, 808–818. [PubMed: 25435138]

Dudziak D, Kamphorst AO, Heidkamp GF, Buchholz VR, Trumpfheller C, Yamazaki S, Cheong C, Liu K, Lee HW, Park CG, et al. (2007). Differential antigen processing by dendritic cell subsets in vivo. Science 315, 107–111. [PubMed: 17204652]

Durai V, and Murphy KM (2016). Functions of Murine Dendritic Cells. Immunity 45, 719–736. [PubMed: 27760337]

Eisenbarth SC (2019). Dendritic cell subsets in T cell programming: location dictates function. Nat. Rev. Immunol 19, 89–103. [PubMed: 30464294]

ElTanbouly MA, Zhao Y, Nowak E, Li J, Schaafsma E, Le Mercier I, Ceeraz S, Lines JL, Peng C, Carriere C, et al. (2020). VISTA is a checkpoint regulator for naïve T cell quiescence and peripheral tolerance. Science 367, eaay0524. [PubMed: 31949051]

Esterházy D, Canesso MCC, Mesin L, Muller PA, de Castro TBR, Lockhart A, ElJalby M, Faria AMC, and Mucida D (2019). Compartmentalized gut lymph node drainage dictates adaptive immune responses. Nature 569, 126–130. [PubMed: 30988509]

Ferris ST, Durai V, Wu R, Theisen DJ, Ward JP, Bern MD, Davidson JT 4th, Bagadia P, Liu T, Briseño CG, et al. (2020). cDC1 prime and are licensed by $CD4^+$ T cells to induce anti-tumour immunity. Nature 584, 624–629. [PubMed: 32788723]

Fontenot JD, Rasmussen JP, Gavin MA, and Rudensky AY (2005). A function for interleukin 2 in Foxp3-expressing regulatory T cells. Nat. Immunol 6, 1142–1151. [PubMed: 16227984]

Francisco LM, Salinas VH, Brown KE, Vanguri VK, Freeman GJ, Kuchroo VK, and Sharpe AH (2009). PD-L1 regulates the development, maintenance, and function of induced regulatory T cells. J. Exp. Med 206, 3015–3029. [PubMed: 20008522]

Freese NH, Norris DC, and Loraine AE (2016). Integrated genome browser: visual analytics platform for genomics. Bioinformatics 32, 2089–2095. [PubMed: 27153568]

Fulton RB, Hamilton SE, Xing Y, Best JA, Goldrath AW, Hogquist KA, and Jameson SC (2015). The TCR's sensitivity to self peptide-MHC dictates the ability of naive CD8(+) T cells to respond to foreign antigens. Nat. Immunol 16, 107–117. [PubMed: 25419629]

Geltink RIK, Kyle RL, and Pearce EL (2018). Unraveling the Complex Interplay Between T Cell Metabolism and Function. Annu. Rev. Immunol 36, 461–488. [PubMed: 29677474]

Gomez JA, Wapinski OL, Yang YW, Bureau JF, Gopinath S, Monack DM, Chang HY, Brahic M, and Kirkegaard K (2013). The NeST long ncRNA controls microbial susceptibility and epigenetic activation of the inter-feron-g locus. Cell 152, 743–754. [PubMed: 23415224]

González-Mariscal L, Miranda J, Raya-Sandino A, Domínguez-Calderón A, and Cuellar-Perez F (2017). ZO-2, a tight junction protein involved in gene expression, proliferation, apoptosis, and cell size regulation. Ann. N Y Acad. Sci 1397, 35–53. [PubMed: 28415133]

Groom JR, Richmond J, Murooka TT, Sorensen EW, Sung JH, Bankert K, von Andrian UH, Moon JJ, Mempel TR, and Luster AD (2012). CXCR3 chemokine receptor-ligand interactions in the lymph node optimize CD4+ T helper 1 cell differentiation. Immunity 37, 1091–1103. [PubMed: 23123063]

Guilliams M, Dutertre CA, Scott CL, McGovern N, Sichien D, Chakarov S, Van Gassen S, Chen J, Poidinger M, De Prijck S, et al. (2016). Unsupervised High-Dimensional Analysis Aligns Dendritic Cells across Tissues and Species. Immunity 45, 669–684. [PubMed: 27637149]

Guo L, Ding Z, Huang N, Huang Z, Zhang N, and Xia Z (2017). Forkhead Box M1 positively regulates UBE2C and protects glioma cells from autophagic death. Cell Cycle 16, 1705–1718. [PubMed: 28767320]

Haftmann C, Stittrich AB, Zimmermann J, Fang Z, Hradilkova K, Bardua M, Westendorf K, Heinz GA, Riedel R, Siede J, et al. (2015). miR-148a is upregulated by Twist1 and T-bet and promotes Th1-cell survival by regulating the proapoptotic gene Bim. Eur. J. Immunol 45, 1192–1205. [PubMed: 25486906]

Han S, Williams S, and Mustelin T (2000). Cytoskeletal protein tyrosine phosphatase PTPH1 reduces T cell antigen receptor signaling. Eur. J. Immunol 30, 1318–1325. [PubMed: 10820377]

Harada Y, Harada Y, Elly C, Ying G, Paik JH, DePinho RA, and Liu YC (2010). Transcription factors Foxo3a and Foxo1 couple the E3 ligase Cbl-b to the induction of Foxp3 expression in induced regulatory T cells. J. Exp. Med 207, 1381–1391. [PubMed: 20439537]

Hawiger D, Inaba K, Dorsett Y, Guo M, Mahnke K, Rivera M, Ravetch JV, Steinman RM, and Nussenzweig MC (2001). Dendritic cells induce peripheral T cell unresponsiveness under steady state conditions in vivo. J. Exp. Med 194, 769–779. [PubMed: 11560993]

Hawiger D, Masilamani RF, Bettelli E, Kuchroo VK, and Nussenzweig MC (2004). Immunological unresponsiveness characterized by increased expression of CD5 on peripheral T cells induced by dendritic cells in vivo. Immunity 20, 695–705. [PubMed: 15189735]

Hawiger D, Wan YY, Eynon EE, and Flavell RA (2010). The transcription cofactor Hopx is required for regulatory T cell function in dendritic cell-mediated peripheral T cell unresponsiveness. Nat. Immunol 11, 962–968. [PubMed: 20802482]

Haxhinasto S, Mathis D, and Benoist C (2008). The AKT-mTOR axis regulates de novo differentiation of CD4+Foxp3+ cells. J. Exp. Med 205, 565–574. [PubMed: 18283119]

He W, Wang C, Mu R, Liang P, Huang Z, Zhang J, and Dong L (2017). MiR-21 is required for anti-tumor immune response in mice: an implication for its bi-directional roles. Oncogene 36, 4212–4223. [PubMed: 28346427]

Henderson JG, Opejin A, Jones A, Gross C, and Hawiger D (2015). CD5 instructs extrathymic regulatory T cell development in response to self and tolerizing antigens. Immunity 42, 471–483. [PubMed: 25786177]

Hirota K, Duarte JH, Veldhoen M, Hornsby E, Li Y, Cua DJ, Ahlfors H, Wilhelm C, Tolaini M, Menzel U, et al. (2011). Fate mapping of IL-17-producing T cells in inflammatory responses. Nat. Immunol 12, 255–263. [PubMed: 21278737]

Homer N (2011). TMAP: The Torrent Mapping Program (Ion Torrent Systems, Inc). https://github.com/iontorrent/TMAP/blob/master/doc/tmap-book.pdf.

Huang N, and Perl A (2018). Metabolism as a Target for Modulation in Autoimmune Diseases. Trends Immunol. 39, 562–576. [PubMed: 29739666]

Huang CT, Huso DL, Lu Z, Wang T, Zhou G, Kennedy EP, Drake CG, Morgan DJ, Sherman LA, Higgins AD, et al. (2003). CD4+ T cells pass through an effector phase during the process of in vivo tolerance induction. J. Immunol 170, 3945–3953. [PubMed: 12682221]

Iberg CA, and Hawiger D (2019). Advancing immunomodulation by in vivo antigen delivery to DEC-205 and other cell surface molecules using recombinant chimeric antibodies. Int. Immunopharmacol 73, 575–580. [PubMed: 31228685]

Iberg CA, and Hawiger D (2020a). Natural and Induced Tolerogenic Dendritic Cells. J. Immunol 204, 733–744. [PubMed: 32015076]

Iberg CA, and Hawiger D (2020b). Targeting Dendritic Cells with Antigen-Delivering Antibodies for Amelioration of Autoimmunity in Animal Models of Multiple Sclerosis and Other Autoimmune Diseases. Antibodies (Basel) 9, 23.

Iberg CA, Jones A, and Hawiger D (2017). Dendritic Cells As Inducers of Peripheral Tolerance. Trends Immunol. 38, 793–804. [PubMed: 28826942]

Ichiyama K, Gonzalez-Martin A, Kim BS, Jin HY, Jin W, Xu W, Sabouri-Ghomi M, Xu S, Zheng P, Xiao C, and Dong C (2016). The MicroRNA-183-96-182 Cluster Promotes T Helper 17 Cell Pathogenicity by Negatively Regulating Transcription Factor Foxo1 Expression. Immunity 44, 1284–1298. [PubMed: 27332731]

Iwasaki A, and Medzhitov R (2015). Control of adaptive immunity by the innate immune system. Nat. Immunol 16, 343–353. [PubMed: 25789684]

Jiang A, Bloom O, Ono S, Cui W, Unternaehrer J, Jiang S, Whitney JA, Connolly J, Banchereau J, and Mellman I (2007). Disruption of E-cadherin-mediated adhesion induces a functionally distinct pathway of dendritic cell maturation. Immunity 27, 610–624. [PubMed: 17936032]

Jones A, and Hawiger D (2017). Peripherally Induced Regulatory T Cells: Recruited Protectors of the Central Nervous System against Autoimmune Neuroinflammation. Front. Immunol 8, 532. [PubMed: 28536579]

Jones A, Opejin A, Henderson JG, Gross C, Jain R, Epstein JA, Flavell RA, and Hawiger D (2015). Peripherally Induced Tolerance Depends on Peripheral Regulatory T Cells That Require Hopx To Inhibit Intrinsic IL-2 Expression. J. Immunol 195, 1489–1497. [PubMed: 26170384]

Jones A, Bourque J, Kuehm L, Opejin A, Teague RM, Gross C, and Hawiger D (2016). Immunomodulatory Functions of BTLA and HVEM Govern Induction of Extrathymic Regulatory T Cells and Tolerance by Dendritic Cells. Immunity 45, 1066–1077. [PubMed: 27793593]

Josefowicz SZ, Lu LF, and Rudensky AY (2012). Regulatory T cells: mechanisms of differentiation and function. Annu. Rev. Immunol 30, 531–564. [PubMed: 22224781]

Kawabe T, Jankovic D, Kawabe S, Huang Y, Lee PH, Yamane H, Zhu J, Sher A, Germain RN, and Paul WE (2017). Memory-phenotype $CD4^+$ T cells spontaneously generated under steady-state

conditions exert innate T_H1-like effector function. Sci. Immunol 2, eaam9304. [PubMed: 28783663]

Kreienkamp R, Graziano S, Coll-Bonfill N, Bedia-Diaz G, Cybulla E, Vindigni A, Dorsett D, Kubben N, Batista LFZ, and Gonzalo S (2018). A Cell-Intrinsic Interferon-like Response Links Replication Stress to Cellular Aging Caused by Progerin. Cell Rep. 22, 2006–2015. [PubMed: 29466729]

Krishnan S, Warke VG, Nambiar MP, Tsokos GC, and Farber DL (2003). The FcR gamma subunit and Syk kinase replace the CD3 zeta-chain and ZAP-70 kinase in the TCR signaling complex of human effector CD4 T cells. J. Immunol 170, 4189–4195. [PubMed: 12682251]

Lee PP, Fitzpatrick DR, Beard C, Jessup HK, Lehar S, Makar KW, Pérez-Melgosa M, Sweetser MT, Schlissel MS, Nguyen S, et al. (2001). A critical role for Dnmt1 and DNA methylation in T cell development, function, and survival. Immunity 15, 763–774. [PubMed: 11728338]

Lee Y, Awasthi A, Yosef N, Quintana FJ, Xiao S, Peters A, Wu C, Kleinewietfeld M, Kunder S, Hafler DA, et al. (2012). Induction and molecular signature of pathogenic TH17 cells. Nat. Immunol 13, 991–999. [PubMed: 22961052]

Li H, Handsaker B, Wysoker A, Fennell T, Ruan J, Homer N, Marth G, Abecasis G, and Durbin R; 1000 Genome Project Data Processing Subgroup (2009). The Sequence Alignment/Map format and SAMtools. Bioinformatics 25, 2078–2079. [PubMed: 19505943]

Li H, Nourbakhsh B, Ciric B, Zhang GX, and Rostami A (2010). Neutralization of IL-9 ameliorates experimental autoimmune encephalomyelitis by decreasing the effector T cell population. J. Immunol 185, 4095–4100. [PubMed: 20805418]

Li X, Acuff NV, Peeks AR, Kirkland R, Wyatt KD, Nagy T, and Watford WT (2016). Tumor Progression Locus 2 (Tpl2) Activates the Mammalian Target of Rapamycin (mTOR) Pathway, Inhibits Forkhead Box P3 (FoxP3) Expression, and Limits Regulatory T Cell (Treg) Immunosuppressive Functions. J. Biol. Chem 291, 16802–16815. [PubMed: 27261457]

Lighvani AA, Frucht DM, Jankovic D, Yamane H, Aliberti J, Hissong BD, Nguyen BV, Gadina M, Sher A, Paul WE, and O'Shea JJ (2001). T-bet is rapidly induced by interferon-gamma in lymphoid and myeloid cells. Proc. Natl. Acad. Sci. USA 98, 15137–15142. [PubMed: 11752460]

Lin CC, Bradstreet TR, Schwarzkopf EA, Sim J, Carrero JA, Chou C, Cook LE, Egawa T, Taneja R, Murphy TL, et al. (2014). Bhlhe40 controls cytokine production by T cells and is essential for pathogenicity in autoimmune neuroinflammation. Nat. Commun 5, 3551. [PubMed: 24699451]

Lippert E, Yowe DL, Gonzalo JA, Justice JP, Webster JM, Fedyk ER, Hodge M, Miller C, Gutierrez-Ramos JC, Borrego F, et al. (2003). Role of regulator of G protein signaling 16 in inflammation-induced T lymphocyte migration and activation. J. Immunol 171, 1542–1555. [PubMed: 12874248]

Liston A, Kohler RE, Townley S, Haylock-Jacobs S, Comerford I, Caon AC, Webster J, Harrison JM, Swann J, Clark-Lewis I, et al. (2009). Inhibition of CCR6 function reduces the severity of experimental autoimmune encephalomyelitis via effects on the priming phase of the immune response. J. Immunol 182, 3121–3130. [PubMed: 19234209]

Long M, Slaiby AM, Wu S, Hagymasi AT, Mihalyo MA, Bandyopadhyay S, Vella AT, and Adler AJ (2007). Histone acetylation at the Ifng promoter in tolerized CD4 cells is associated with increased IFN-gamma expression during subsequent immunization to the same antigen. J. Immunol 179, 5669–5677. [PubMed: 17947638]

Lund R, Ahlfors H, Kainonen E, Lahesmaa AM, Dixon C, and Lahesmaa R (2005). Identification of genes involved in the initiation of human Th1 or Th2 cell commitment. Eur. J. Immunol 35, 3307–3319. [PubMed: 16220538]

Mandl JN, Monteiro JP, Vrisekoop N, and Germain RN (2013). T cell-positive selection uses self-ligand binding strength to optimize repertoire recognition of foreign antigens. Immunity 38, 263–274. [PubMed: 23290521]

Manicassamy S, Reizis B, Ravindran R, Nakaya H, Salazar-Gonzalez RM, Wang YC, and Pulendran B (2010). Activation of beta-catenin in dendritic cells regulates immunity versus tolerance in the intestine. Science 329, 849–853. [PubMed: 20705860]

Mariotto A, Pavlova O, Park HS, Huber M, and Hohl D (2016). HOPX: The Unusual Homeodomain-Containing Protein. J. Invest. Dermatol 136, 905–911. [PubMed: 27017330]

Martin B, Auffray C, Delpoux A, Pommier A, Durand A, Charvet C, Yakonowsky P, de Boysson H, Bonilla N, Audemard A, et al. (2013). Highly self-reactive naive CD4 T cells are prone to differentiate into regulatory T cells. Nat. Commun 4, 2209. [PubMed: 23900386]

Martínez-Barricarte R, Markle JG, Ma CS, Deenick EK, Ramírez-Alejo N, Mele F, Latorre D, Mahdaviani SA, Aytekin C, Mansouri D, et al. (2018). Human IFN-γ immunity to mycobacteria is governed by both IL-12 and IL-23. Sci. Immunol 3, eaau6759. [PubMed: 30578351]

Martínez-Llordella M, Esensten JH, Bailey-Bucktrout SL, Lipsky RH, Marini A, Chen J, Mughal M, Mattson MP, Taub DD, and Bluestone JA (2013). CD28-inducible transcription factor DEC1 is required for efficient autoreactive CD4+ T cell response. J. Exp. Med 210, 1603–1619. [PubMed: 23878307]

Mendes-da-Cruz DA, Brignier AC, Asnafi V, Baleydier F, Messias CV, Lepelletier Y, Bedjaoui N, Renand A, Smaniotto S, Canioni D, et al. (2014). Semaphorin 3F and neuropilin-2 control the migration of human T-cell precursors. PLoS ONE 9, e103405. [PubMed: 25068647]

Merad M, Sathe P, Helft J, Miller J, and Mortha A (2013). The dendritic cell lineage: ontogeny and function of dendritic cells and their subsets in the steady state and the inflamed setting. Annu. Rev. Immunol 31, 563–604. [PubMed: 23516985]

Midorikawa R, Takei Y, and Hirokawa N (2006). KIF4 motor regulates activity-dependent neuronal survival by suppressing PARP-1 enzymatic activity. Cell 125, 371–383. [PubMed: 16630823]

Mombaerts P, Iacomini J, Johnson RS, Herrup K, Tonegawa S, and Papaioannou VE (1992). RAG-1-deficient mice have no mature B and T lymphocytes. Cell 68, 869–877. [PubMed: 1547488]

Moschovakis GL, Bubke A, Friedrichsen M, Falk CS, Feederle R, and Förster R (2017). T cell specific Cxcr5 deficiency prevents rheumatoid arthritis. Sci. Rep 7, 8933. [PubMed: 28827539]

Murugaiyan G, da Cunha AP, Ajay AK, Joller N, Garo LP, Kumaradevan S, Yosef N, Vaidya VS, and Weiner HL (2015). MicroRNA-21 promotes Th17 differentiation and mediates experimental autoimmune encephalomyelitis. J. Clin. Invest 125, 1069–1080. [PubMed: 25642768]

Naik S, Bouladoux N, Wilhelm C, Molloy MJ, Salcedo R, Kastenmuller W, Deming C, Quinones M, Koo L, Conlan S, et al. (2012). Compartmentalized control of skin immunity by resident commensals. Science 337, 1115–1119. [PubMed: 22837383]

Nowak EC, Weaver CT, Turner H, Begum-Haque S, Becher B, Schreiner B, Coyle AJ, Kasper LH, and Noelle RJ (2009). IL-9 as a mediator of Th17-driven inflammatory disease. J. Exp. Med 206, 1653–1660. [PubMed: 19596803]

O'Sullivan D, and Pearce EL (2015). Targeting T cell metabolism for therapy. Trends Immunol. 36, 71–80. [PubMed: 25601541]

Olesin E, Nayar R, Saikumar-Lakshmi P, and Berg LJ (2018). The Transcription Factor Runx2 Is Required for Long-Term Persistence of Antiviral $CD8^+$ Memory T Cells. Immunohorizons 2, 251–261. [PubMed: 30264035]

Ouyang W, Beckett O, Ma Q, Paik JH, DePinho RA, and Li MO (2010). Foxo proteins cooperatively control the differentiation of Foxp3+ regulatory T cells. Nat. Immunol 11, 618–627. [PubMed: 20467422]

Persaud SP, Parker CR, Lo WL, Weber KS, and Allen PM (2014). Intrinsic CD4+ T cell sensitivity and response to a pathogen are set and sustained by avidity for thymic and peripheral complexes of self peptide and MHC. Nat. Immunol 15, 266–274. [PubMed: 24487322]

Petermann F, Pekowska A, Johnson CA, Jankovic D, Shih HY, Jiang K, Hudson WH, Brooks SR, Sun HW, Villarino AV, et al. (2019). The Magnitude of IFN-γ Responses Is Fine-Tuned by DNA Architecture and the Non-coding Transcript of Ifng-as1. Mol. Cell 75, 1229–1242.e5. [PubMed: 31377117]

Peters VA, Joesting JJ, and Freund GG (2013). IL-1 receptor 2 (IL-1R2) and its role in immune regulation. Brain Behav. Immun 32, 1–8. [PubMed: 23195532]

Peterson TR, Sengupta SS, Harris TE, Carmack AE, Kang SA, Balderas E, Guertin DA, Madden KL, Carpenter AE, Finck BN, and Sabatini DM (2011). mTOR complex 1 regulates lipin 1 localization to control the SREBP pathway. Cell 146, 408–420. [PubMed: 21816276]

Platten M, Youssef S, Hur EM, Ho PP, Han MH, Lanz TV, Phillips LK, Goldstein MJ, Bhat R, Raine CS, et al. (2009). Blocking angiotensin-converting enzyme induces potent regulatory T cells and

modulates TH1- and TH17-mediated autoimmunity. Proc. Natl. Acad. Sci. USA 106, 14948–14953. [PubMed: 19706421]

Pulendran B (2015). The varieties of immunological experience: of pathogens, stress, and dendritic cells. Annu. Rev. Immunol 33, 563–606. [PubMed: 25665078]

Quinlan AR, and Hall IM (2010). BEDTools: a flexible suite of utilities for comparing genomic features. Bioinformatics 26, 841–842. [PubMed: 20110278]

Quintana FJ, Basso AS, Iglesias AH, Korn T, Farez MF, Bettelli E, Caccamo M, Oukka M, and Weiner HL (2008). Control of T(reg) and T(H) 17 cell differentiation by the aryl hydrocarbon receptor. Nature 453, 65–71. [PubMed: 18362915]

Razawy W, Asmawidjaja PS, Mus AM, Salioska N, Davelaar N, Kops N, Oukka M, Alves CH, and Lubberts E (2020). $CD4^+$ $CCR6^+$ T cells, but not gammadelta T cells, are important for the IL-23R-dependent progression of antigen-induced inflammatory arthritis in mice. Eur. J. Immunol 50, 245–255. [PubMed: 31778214]

R Development Core Team (2015). R: a language and environment for statistical computing (R Foundation for Statistical Computing).

Sancho D, and Reis e Sousa C (2012). Signaling by myeloid C-type lectin receptors in immunity and homeostasis. Annu. Rev. Immunol 30, 491–529. [PubMed: 22224766]

Sauer S, Bruno L, Hertweck A, Finlay D, Leleu M, Spivakov M, Knight ZA, Cobb BS, Cantrell D, O'Connor E, et al. (2008). T cell receptor signaling controls Foxp3 expression via PI3K, Akt, and mTOR. Proc. Natl. Acad. Sci. USA 105, 7797–7802. [PubMed: 18509048]

Scalzo-Inguanti K, and Plebanski M (2011). CD38 identifies a hypo-proliferative IL-13-secreting CD4+ T-cell subset that does not fit into existing naive and memory phenotype paradigms. Eur. J. Immunol 41, 1298–1308. [PubMed: 21469087]

Schulz EG, Mariani L, Radbruch A, and Höfer T (2009). Sequential polarization and imprinting of type 1 T helper lymphocytes by interferon-gamma and interleukin-12. Immunity 30, 673–683. [PubMed: 19409816]

Sedy JR, Gavrieli M, Potter KG, Hurchla MA, Lindsley RC, Hildner K, Scheu S, Pfeffer K, Ware CF, Murphy TL, and Murphy KM (2005). B and T lymphocyte attenuator regulates T cell activation through interaction with herpesvirus entry mediator. Nat. Immunol 6, 90–98. [PubMed: 15568026]

Segura E, and Amigorena S (2013). Inflammatory dendritic cells in mice and humans. Trends Immunol. 34, 440–445. [PubMed: 23831267]

Serroukh Y, Gu-Trantien C, Hooshiar Kashani B, Defrance M, Vu Manh TP, Azouz A, Detavernier A, Hoyois A, Das J, Bizet M, et al. (2018). The transcription factors Runx3 and ThPOK cross-regulate acquisition of cytotoxic function by human Th1 lymphocytes. eLife 7, e30496. [PubMed: 29488879]

Shao X, Chen S, Yang D, Cao M, Yao Y, Wu Z, Li N, Shen N, Li X, Song X, and Qian Y (2017). FGF2 cooperates with IL-17 to promote autoimmune inflammation. Sci. Rep 7, 7024. [PubMed: 28765647]

Shin CH, Liu ZP, Passier R, Zhang CL, Wang DZ, Harris TM, Yamagishi H, Richardson JA, Childs G, and Olson EN (2002). Modulation of cardiac growth and development by HOP, an unusual homeodomain protein. Cell 110, 725–735. [PubMed: 12297046]

Shnyreva M, Weaver WM, Blanchette M, Taylor SL, Tompa M, Fitzpatrick DR, and Wilson CB (2004). Evolutionarily conserved sequence elements that positively regulate IFN-gamma expression in T cells. Proc. Natl. Acad. Sci. USA 101, 12622–12627. [PubMed: 15304658]

Sood A, Lebel ME, Fournier M, Rogers D, Mandl JN, and Melichar HJ (2019). Differential interferon-gamma production potential among naïve $CD4^+$ T cells exists prior to antigen encounter. Immunol. Cell Biol 97, 931–940. [PubMed: 31420892]

Sozio MS, Mathis MA, Young JA, Wälchli S, Pitcher LA, Wrage PC, Bartók B, Campbell A, Watts JD, Aebersold R, et al. (2004). PTPH1 is a predominant protein-tyrosine phosphatase capable of interacting with and dephosphorylating the T cell receptor zeta subunit. J. Biol. Chem 279, 7760–7769. [PubMed: 14672952]

Steinman RM (1996). Dendritic cells and immune-based therapies. Exp. Hematol 24, 859–862. [PubMed: 8690042]

Steinman RM (2007). Dendritic cells: understanding immunogenicity. Eur. J. Immunol 37 (Suppl 1), S53–S60. [PubMed: 17972346]

Steinman RM (2012). Decisions about dendritic cells: past, present, and future. Annu. Rev. Immunol 30, 1–22. [PubMed: 22136168]

Steinman RM, Hawiger D, and Nussenzweig MC (2003). Tolerogenic dendritic cells. Annu. Rev. Immunol 21, 685–711. [PubMed: 12615891]

Storey JD, and Tibshirani R (2003). Statistical significance for genomewide studies. Proc. Natl. Acad. Sci. USA 100, 9440–9445. [PubMed: 12883005]

Subramanian A, Tamayo P, Mootha VK, Mukherjee S, Ebert BL, Gillette MA, Paulovich A, Pomeroy SL, Golub TR, Lander ES, and Mesirov JP (2005). Gene set enrichment analysis: a knowledge-based approach for interpreting genome-wide expression profiles. Proc. Natl. Acad. Sci. USA 102, 15545–15550. [PubMed: 16199517]

Sun CM, Hall JA, Blank RB, Bouladoux N, Oukka M, Mora JR, and Belkaid Y (2007). Small intestine lamina propria dendritic cells promote de novo generation of Foxp3 T reg cells via retinoic acid. J. Exp. Med 204, 1775–1785. [PubMed: 17620362]

Swain A, Misulovin Z, Pherson M, Gause M, Mihindukulasuriya K, Rick-els RA, Shilatifard A, and Dorsett D (2016). Drosophila TDP-43 RNA-Binding Protein Facilitates Association of Sister Chromatid Cohesion Proteins with Genes, Enhancers and Polycomb Response Elements. PLoS Genet. 12, e1006331. [PubMed: 27662615]

Takeda N, Jain R, Leboeuf MR, Padmanabhan A, Wang Q, Li L, Lu MM, Millar SE, and Epstein JA (2013). Hopx expression defines a subset of multipotent hair follicle stem cells and a progenitor population primed to give rise to K6+ niche cells. Development 140, 1655–1664. [PubMed: 23487314]

Tello-Lafoz M, Martínez-Martínez G, Rodríguez-Rodríguez C, Albar JP, Huse M, Gharbi S, and Merida I (2017). Sorting nexin 27 interactome in T-lymphocytes identifies zona occludens-2 dynamic redistribution at the immune synapse. Traffic 18, 491–504. [PubMed: 28477369]

Uzawa A, Mori M, Taniguchi J, and Kuwabara S (2014). Modulation of the kallikrein/kinin system by the angiotensin-converting enzyme inhibitor alleviates experimental autoimmune encephalomyelitis. Clin. Exp. Immunol 178, 245–252. [PubMed: 24996009]

van Panhuys N, Klauschen F, and Germain RN (2014). T-cell-receptor-dependent signal intensity dominantly controls CD4(+) T cell polarization In Vivo. Immunity 41, 63–74. [PubMed: 24981853]

Vander Lugt B, Riddell J, Khan AA, Hackney JA, Lesch J, DeVoss J, Weirauch MT, Singh H, and Mellman I (2017). Transcriptional determinants of tolerogenic and immunogenic states during dendritic cell maturation. J. Cell Biol 216, 779–792. [PubMed: 28130292]

Vokali E, Yu SS, Hirosue S, Rinçon-Restrepo M, Duraes FV, Scherer S, Corthésy-Henrioud P, Kilarski WW, Mondino A, Zehn D, et al. (2020). Lymphatic endothelial cells prime naı¨ve $CD8^+$ T cells into memory cells under steady-state conditions. Nat. Commun 11, 538. [PubMed: 31988323]

Wan YY, and Flavell RA (2005). Identifying Foxp3-expressing suppressor T cells with a bicistronic reporter. Proc. Natl. Acad. Sci. USA 102, 5126–5131. [PubMed: 15795373]

Wang L, Pino-Lagos K, de Vries VC, Guleria I, Sayegh MH, and Noelle RJ (2008). Programmed death 1 ligand signaling regulates the generation of adaptive Foxp3+CD4+ regulatory T cells. Proc. Natl. Acad. Sci. USA 105, 9331–9336. [PubMed: 18599457]

Wang C, Collins M, and Kuchroo VK (2015). Effector T cell differentiation: are master regulators of effector T cells still the masters? Curr. Opin. Immunol 37, 6–10. [PubMed: 26319196]

Warth SC, Hoefig KP, Hiekel A, Schallenberg S, Jovanovic K, Klein L, Kretschmer K, Ansel KM, and Heissmeyer V (2015). Induced miR-99a expression represses Mtor cooperatively with miR-150 to promote regulatory T-cell differentiation. EMBO J. 34, 1195–1213. [PubMed: 25712478]

Weatherly K, Bettonville M, Torres D, Kohler A, Goriely S, and Braun MY (2015). Functional profile of S100A4-deficient T cells. Immun. Inflamm. Dis 3, 431–444. [PubMed: 26734465]

Webb GJ, Hirschfield GM, and Lane PJ (2016). OX40, OX40L and Auto-immunity: a Comprehensive Review. Clin. Rev. Allergy Immunol 50, 312–332. [PubMed: 26215166]

Wieland GD, Nehmann N, Müller D, Eibel H, Siebenlist U, Sühnel J, Zipfel PF, and Skerka C (2005). Early growth response proteins EGR-4 and EGR-3 interact with immune inflammatory mediators NF-kappaB p50 and p65. J. Cell Sci 118, 3203–3212. [PubMed: 16014385]

Wu L, Hollinshead KER, Hao Y, Au C, Kroehling L, Ng C, Lin WY, Li D, Silva HM, Shin J, et al. (2020). Niche-Selective Inhibition of Pathogenic Th17 Cells by Targeting Metabolic Redundancy. Cell 182, 641–654.e20. [PubMed: 32615085]

Yan H, Wu L, Shih C, Hou S, Shi J, Mao T, Chen W, Melvin B, Rigby RJ, Chen Y, et al. (2017). Plexin B2 and Semaphorin 4C Guide T Cell Recruitment and Function in the Germinal Center. Cell Rep. 19, 995–1007. [PubMed: 28467912]

Yang K, Shrestha S, Zeng H, Karmaus PW, Neale G, Vogel P, Guertin DA, Lamb RF, and Chi H (2013). T cell exit from quiescence and differentiation into Th2 cells depend on Raptor-mTORC1-mediated metabolic reprogramming. Immunity 39, 1043–1056. [PubMed: 24315998]

Yang CY, Li JP, Chiu LL, Lan JL, Chen DY, Chuang HC, Huang CY, and Tan TH (2014). Dual-specificity phosphatase 14 (DUSP14/MKP6) negatively regulates TCR signaling by inhibiting TAB1 activation. J. Immunol 192, 1547–1557. [PubMed: 24403530]

Yao C, Sakata D, Esaki Y, Li Y, Matsuoka T, Kuroiwa K, Sugimoto Y, and Narumiya S (2009). Prostaglandin E2-EP4 signaling promotes immune inflammation through Th1 cell differentiation and Th17 cell expansion. Nat. Med 15, 633–640. [PubMed: 19465928]

Yatim N, Cullen S, and Albert ML (2017). Dying cells actively regulate adaptive immune responses. Nat. Rev. Immunol 17, 262–275. [PubMed: 28287107]

Zelenay S, and Reis e Sousa C (2013). Adaptive immunity after cell death. Trends Immunol. 34, 329–335. [PubMed: 23608152]

Zeng H, and Chi H (2017). mTOR signaling in the differentiation and function of regulatory and effector T cells. Curr. Opin. Immunol 46, 103–111. [PubMed: 28535458]

Zhang L, Ke F, Liu Z, Bai J, Liu J, Yan S, Xu Z, Lou F, Wang H, Zhu H, et al. (2015a). MicroRNA-31 negatively regulates peripherally derived regulatory T-cell generation by repressing retinoic acid-inducible protein 3. Nat. Commun 6, 7639. [PubMed: 26165721]

Zhang R, Tian A, Wang J, Shen X, Qi G, and Tang Y (2015b). miR26a modulates Th17/T reg balance in the EAE model of multiple sclerosis by targeting IL6. Neuromolecular Med. 17, 24–34. [PubMed: 25362566]

Zhu J (2018). T Helper Cell Differentiation, Heterogeneity, and Plasticity. Cold Spring Harb. Perspect. Biol 10, a030338. [PubMed: 28847903]

Highlights

- Induction of effector precursors is inherent to T cell responses in the steady state
- Effector precursors are programmed for terminal differentiation upon re-stimulation
- cDC2 and functions of mTORC1 in T cells increase induction of effector precursors
- Greater proportion of effector precursors decreases numbers of potential pTreg cells

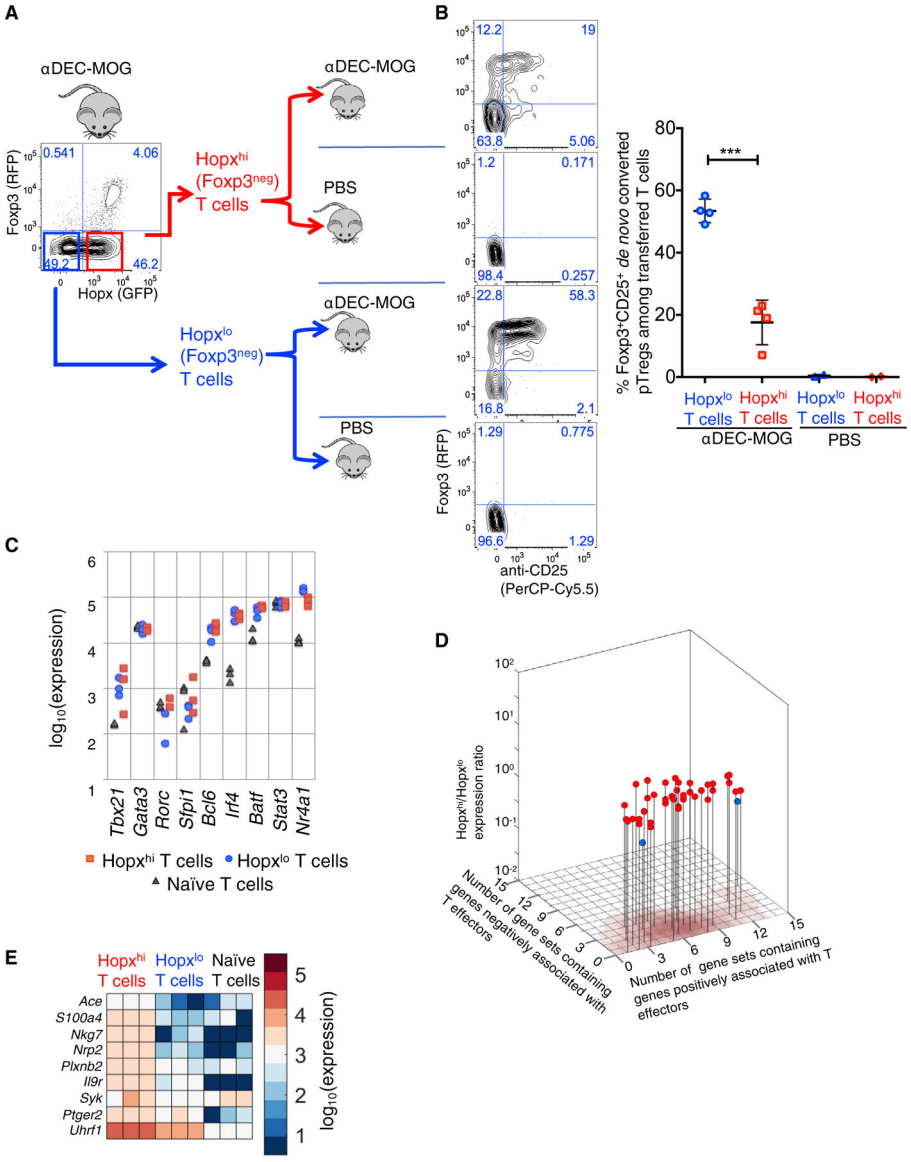

Figure 1. Dendritic Cells Induce Regulatory and Effector-Related T Cells in the Steady State

(A and B) Induction of Hopx^{hi} and Hopx^{lo} T cells that differ in their pTreg cell conversion potential *in vivo*.

(A) General experimental outline for examining Hopx^{hi} and Hopx^{lo} T cells. Plots (representative of multiple independent experiments) show Hopx (GFP) and Foxp3 (RFP) expression, and the corresponding regions indicate gating for automated cell sorting in pooled CD4^{+} T cells combined from peripheral lymph nodes and spleens obtained from MOG-specific TCR tg (2D2) *Hopx^{GFP}Foxp3^{RFP}* mice 5 days after treatment with αDEC-MOG chimeric antibody. Arrows indicate adoptive transfers of Hopx^{hi} and Hopx^{lo} T cells into WT recipient mice that were then treated with either αDEC-MOG or PBS as indicated.

(B) Representative plots show Foxp3 (RFP) expression and anti-CD25 staining intensity in the transferred CD4^{+} T cells among splenocytes from the recipients as in (A) analyzed by flow cytometry after 21 days. Numbers in quadrants show corresponding percentages. Graph

shows mean ± standard deviation (SD) percentages of $Foxp3^{+}CD25^{+}$ pTreg cells among transferred $CD4^{+}$ T cells in the indicated groups of recipients; ***$p < 0.001$ determined by unpaired t test, n = 4 per group from two independent experiments.

(C) Expression of master regulators. The graphs show expression of *Tbx21*, *Gata3*, *Rorc*, *Sfpi1*, *Bcl6*, *Irf4*, *Batf*, *Stat3*, and *Nr4a1* determined by RNA-sequencing (RNA-seq) in multiple independent replicates from the $Hopx^{hi}$, $Hopx^{lo}$, and naive 2D2 T cells obtained as in Figure S1F and analyzed as described in Star Methods. None of those genes have significantly different expression between $Hopx^{hi}$ and $Hopx^{lo}$ T cells.

(D) Gene set enrichment analysis (GSEA). Individual genes whose expression is significantly different between $Hopx^{hi}$ and $Hopx^{lo}$ T cells and that were identified by the GSEA are shown as present in the indicated numbers of publicly available gene sets either positively (containing genes with upregulated expression in effector/memory T cells) or negatively (containing genes with downregulated expression in effector/memory T cells) associated with effector or memory T cells. The vertical axes show the specific ratio of expression of such genes in $Hopx^{hi}$ T cells and $Hopx^{lo}$ T cells, and red and blue dots denote individual genes with either upregulated or downregulated, respectively, expression in $Hopx^{hi}$ T cells in comparison with $Hopx^{lo}$ T cells. A shaded contour represents the distribution of projections of the dots onto the horizontal plane.

(E) Immune gene expression. Heatmap shows expression of additionally identified genes whose expression is significantly different between $Hopx^{hi}$ and $Hopx^{lo}$ T cells and that are associated with specific immune cell functions (see text and Table 1). Multiple independent replicates are shown.

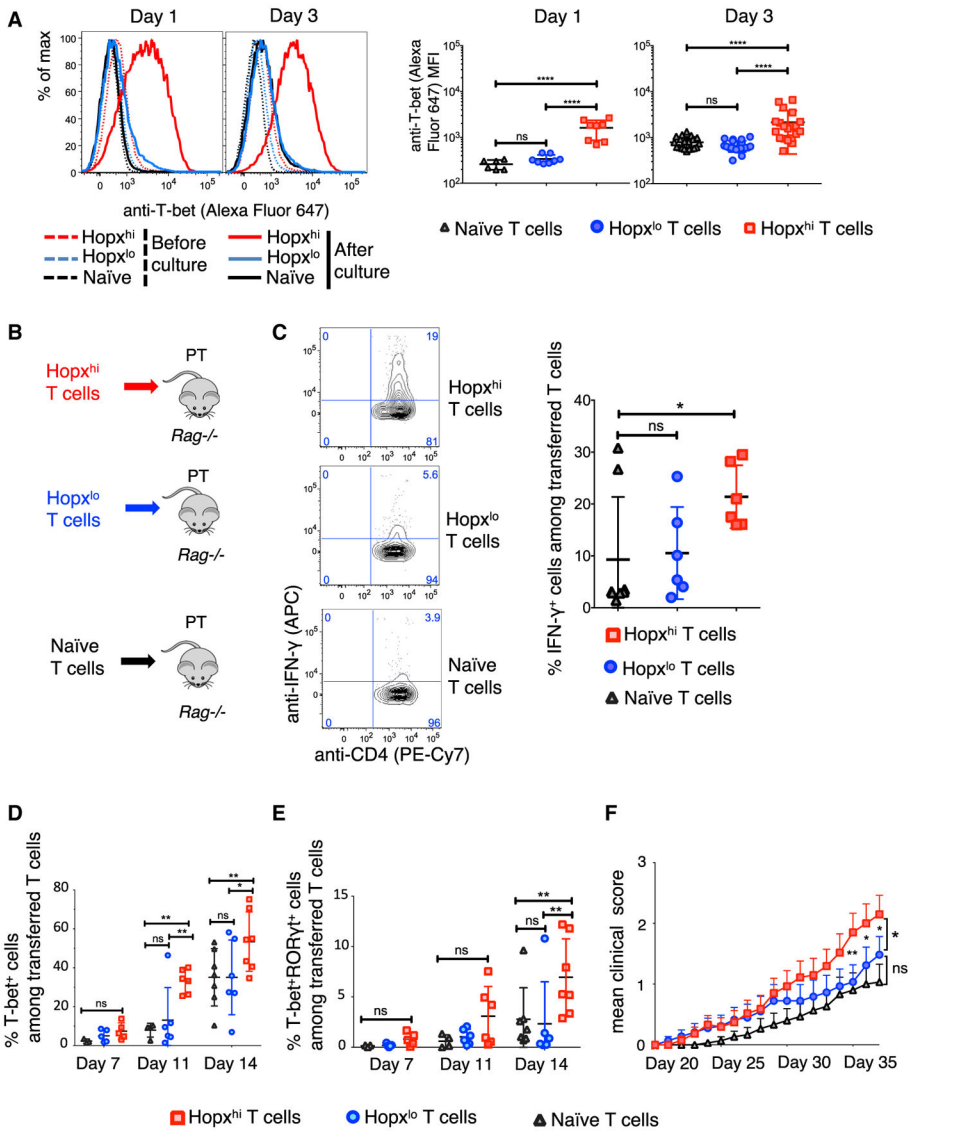

Figure 2. Effector Precursors Undergo Robust Terminal Differentiation *In Vitro* and *In Vivo*

(A) Induction of T-bet expression. Representative histograms show anti-T-bet intracellular staining intensity analyzed by flow cytometry in Hopx^{hi}, Hopx^{lo}, and naive 2D2 T cells that were obtained as in Figure S1F and then re-stimulated *in vitro* under Th0 conditions for either 1 or 3 days as indicated. Graphs show mean ± SD median fluorescence intensity (MFI) in the indicated groups, n = 6–20 replicates from three independent experiments using pooled material from multiple mice per group.

(B) General experimental outline of analyzing the differentiation and functions *in vivo* of the Hopx^{hi}, Hopx^{lo}, and naive 2D2 T cells that were obtained as in Figure S1F and then adoptively transferred into multiple independent groups of *Rag*$^{-/-}$ recipient mice also treated with pertussis toxin (PT).

(C) Induction of IFN-γ expression. Representative plots show anti-CD4 and intracellular anti-IFN-γ staining intensity in the transferred CD4^{+}CD3^{+} T cells among splenocytes

analyzed by flow cytometry after 12 days and then additional re-stimulation *in vitro*. Graphs show mean ± SD percentages of IFN-γ^+ cells among transferred T cells in the indicated groups, n = 5–6 individual mice per group from two independent experiments.

(D–F) Terminal effector differentiation and acquisition of autoimmune functions of $Hopx^{hi}$, $Hopx^{lo}$, and naive T cells that were transferred as in (B).

(D) Graphs show mean ± SD percentages of T-bet^+ cells among transferred T cells in the indicated groups after 7, 11, or 14 days as indicated.

(E) Graphs show mean ± SD percentages of T-$bet^+ROR\gamma t^+$ cells among transferred T cells in the indicated groups after 7, 11, or 14 days as indicated. (D and E) n = 3–7 individual mice per group from three independent experiments.

(F) Graphs show mean ± SEM EAE disease scores in the indicated groups and at the indicated days; n = 25 individual mice per group from five independent experiments.

*p < 0.05, **p < 0.01, ***p < 0.001, ****p < 0.0001, determined by Welch's t test (A and C) or two-way ANOVA with Fisher's least significant difference (LSD) (D–F). ns, not significant.

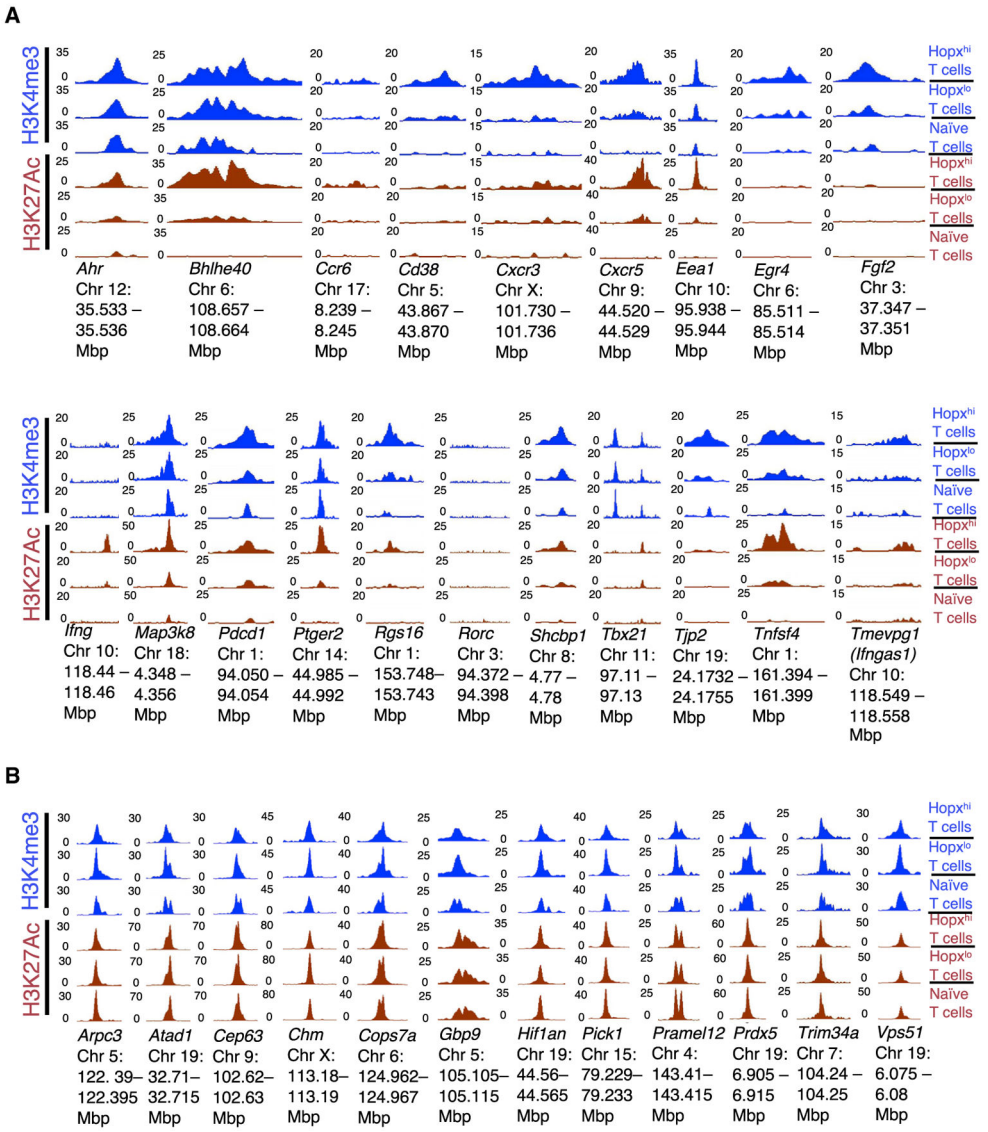

Figure 3. Epigenetic Modifications of T Cell Effector Fate Regulators in Effector Precursors

(A and B) Hopx^{hi}, Hopx^{lo}, and naive 2D2 T cells were obtained as in Figure S1F and analyzed by ChIP-seq. Genomic tracks were calculated from multiple independent experiments and show H3K4me3 and H3K27Ac enrichments for indicated genes or established enhancer regions (in case of *Ifng*) at the given positions in the genome.

(A) Genomic tracks shown for identified relevant regulators of T cell fate.

(B) Genomic tracks shown for select genes with no known functions in T cell differentiation.

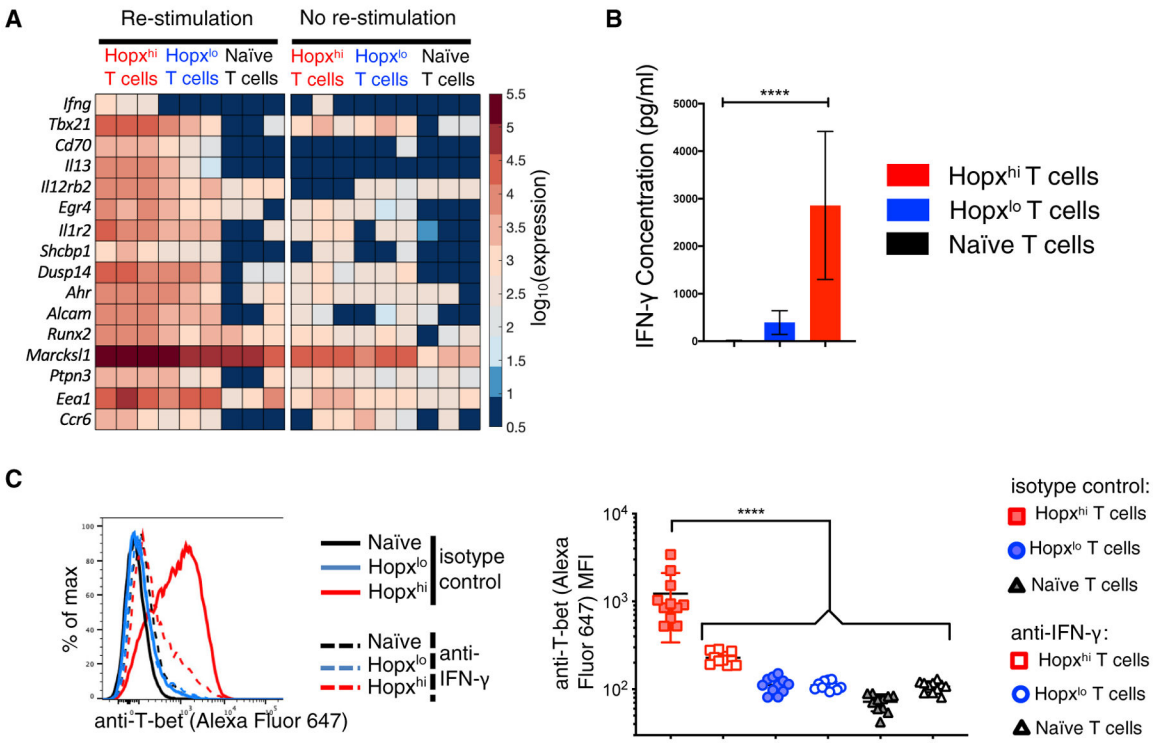

Figure 4. Programmed Expression of Interferon-g in Effector Precursors Mediates an Expression of T-bet

(A and B) Robust induction of *Ifng* expression and IFN-γ production upon re-stimulation.

(A) Hopx^{hi}, Hopx^{lo}, and naive 2D2 T cells were obtained as in Figure S1F and then additionally re-stimulated *in vitro* under Th0 conditions for 12 h as indicated (see Star Methods). RNA-seq heatmaps show expression of T cell-relevant genes whose expression in Hopx^{hi} and Hopx^{lo} T cells was found to be significantly different after the re-stimulation, but not in the absence of re-stimulation. Multiple independent replicates of Hopx^{hi}, Hopx^{lo}, and naive T cell groups are shown.

(B) Hopx^{hi}, Hopx^{lo}, and naive 2D2 T cells were obtained as in Figure S1F and were then cultured *in vitro* under Treg cell-skewing conditions for 4 days. The concentration of IFN-γ was measured in the supernatants at the end of the cultures. Results show mean ± SD MFI in the indicated groups; n = 12–20 replicates from three independent experiments using pooled material from multiple mice per group. ***p < 0.001, determined by Welch's t test.

(C) IFN-γ induces T-bet expression. Representative histograms show anti-T-bet intracellular staining intensity analyzed by flow cytometry in Hopx^{hi}, Hopx^{lo}, and naive 2D2 T cells that were obtained as in Figure S1F and then re-stimulated under Th0 conditions for 3 days in the presence of either anti-IFN-γ or isotype control antibody as indicated. Graphs show mean ± SD MFI in the indicated groups, n = 10–14 replicates from three independent experiments using pooled material from multiple mice per group. ***p < 0.001, determined by Welch's t test.

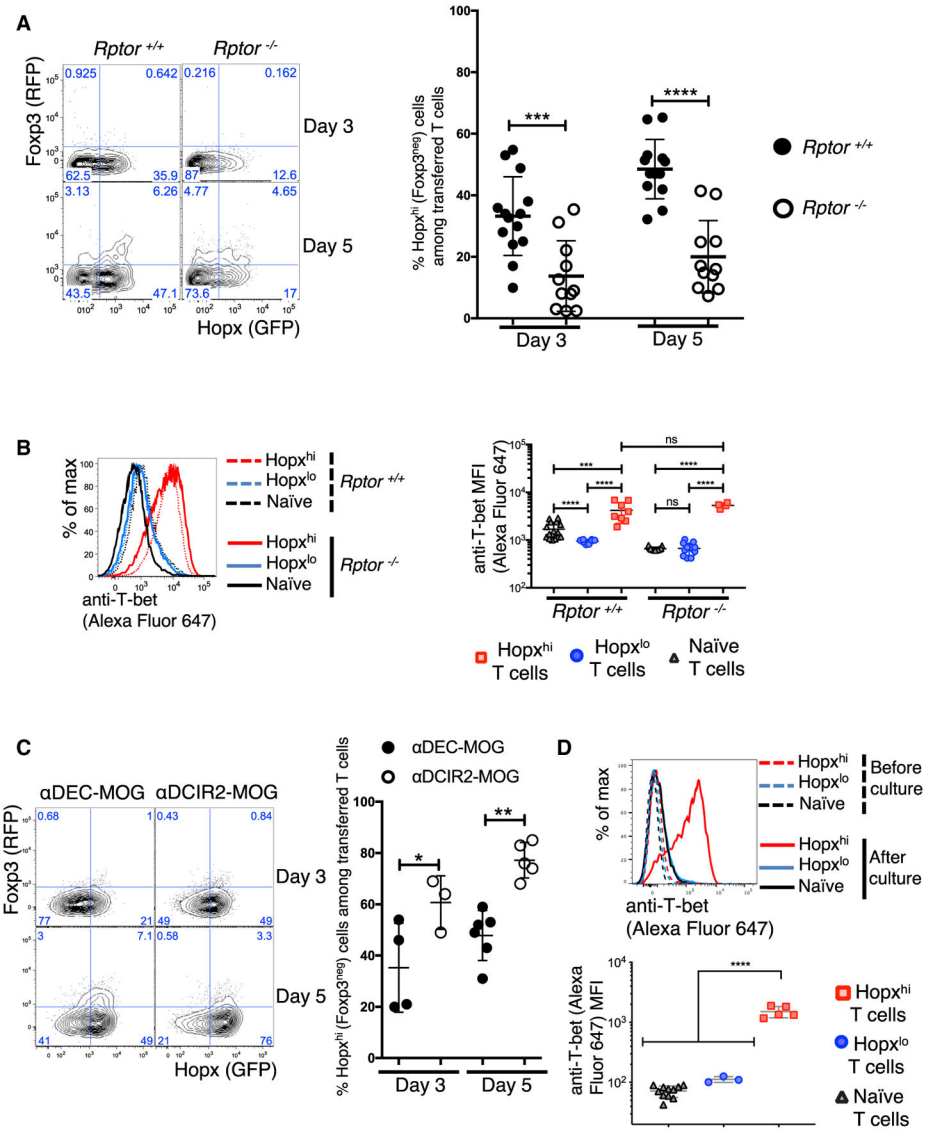

Figure 5. cDC2 and mTORC1 Increase Induction of Effector Precursors

(A) Impact of mTORC1 on the formation of effector precursors. Hopx(GFP)^{neg}Foxp3(RFP)^{neg}CD25^{neg} 2D2 T cells were isolated from *Rptor*$^{-/-}$ and *Rptor*$^{+/+}$ 2D2 *Hopx*^{GFP}*Foxp3*^{RFP} mice and were adoptively transferred into congenically labeled recipient mice that were then treated with αDEC-MOG. Representative plots show Hopx(GFP) and Foxp3(RFP) expression in the transferred CD4^{+} T cells among splenocytes analyzed by flow cytometry after 3 and 5 days as indicated. Numbers in quadrants show corresponding percentages. Graphs show mean ± SD percentages of Hopx^{hi} cells among transferred CD4^{+} T cells in indicated groups of recipients; n = 11–12 individual mice per group from five independent experiments.

(B) Induction of T-bet expression in the absence of mTORC1. Representative histograms show anti-T-bet intracellular staining intensity analyzed by flow cytometry in *Rptor*$^{-/-}$ and *Rptor*$^{+/+}$ Hopx^{hi}, Hopx^{lo}, and naive 2D2 T cells that were obtained as outlined in Figure S1F

from the *Rptor*$^{-/-}$ and *Rptor*$^{+/+}$ 2D2 *Hopx*^{GFP}*Foxp3*^{RFP} mice pre-treated with either αDEC-MOG or PBS. T cells were then re-stimulated *in vitro* under Th0 conditions for 3 days as indicated. Graphs show mean ± SD MFI in the indicated groups; n = 4–15 replicates using pooled material from multiple mice per group from four independent experiments.
(C) Enhanced formation of effector precursors after antigenic stimulation mediated by cDC2. Hopx(GFP)^{neg}Foxp3(RFP)^{neg}CD25^{neg} 2D2 T cells were adoptively transferred into congenically labeled recipient mice that were then treated with either αDEC-MOG or αDCIR2-MOG. Representative plots show Hopx(GFP) and Foxp3(RFP) expression in the transferred CD4^{+} T cells among splenocytes analyzed by flow cytometry after 3 and 5 days as indicated. Numbers in quadrants show corresponding percentages. Graphs show mean ± SD percentages of Hopx^{hi} cells among transferred CD4^{+} T cells in the indicated groups of recipients; n = 3–6 individual mice per group from three independent experiments.
(D) T-bet expression. Representative histograms show anti-T-bet intracellular staining intensity analyzed by flow cytometry in Hopx^{hi}, Hopx^{lo}, and naive 2D2 T cells obtained as outlined in Figure S1F from 2D2 *Hopx*^{GFP}*Foxp3*^{RFP} mice that were pre-treated with αDCIR2-MOG and then re-stimulated *in vitro* under Th0 conditions for 3 days. Graphs show mean ± SD MFI in the indicated groups; n = 3–15 replicates using pooled material from multiple mice per group. Results represent one of two independent experiments.
*p < 0.05, **p < 0.01, ***p < 0.001, ****p < 0.0001, determined by two-way ANOVA with Sidak's multiple comparisons (A and C) or Welch's t test (B and D). ns, not significant.

Table 1.

Genes Related to Effector Differentiation and Functions Specifically Identified in Effector Precursors by Transcriptional and Epigenetic Analyses

Gene	Function
Ace	regulates Th1/Th17 cell cytokine production and migration (Platten et al., 2009; Uzawa et al., 2014)
Ahr	regulates both Treg and Th17 cell differentiation in autoimmune disease (Quintana et al., 2008)
Alcam	regulates $CD4^+$ T cell migration across blood-brain barrier endothelium during EAE (Cayrol et al., 2008)
Aspm	regulates cyclin activity by modulating its phosphorylation and localization into the nucleus (Capecchi and Pozner, 2015)
Bhlhe40	promotes effector T cell differentiation by positively regulating GM-CSF and inhibiting the production of IL-10 (Lin et al., 2014; Martínez-Llordella et al., 2013)
Ccr6	regulates inflammatory T cell priming and lymphoid egress in EAE and arthritis (Liston et al., 2009; Razawy et al., 2020)
Cd38	associated with expression of Th2 effector cytokine IL-13 (Scalzo-Inguanti and Plebanski, 2011)
Cd70	important for T-bet and IFN-γ expression by both Th1 and Th17 effector cells (Dhaeze et al., 2019)
Cdk1	regulates Cdk2/cyclin A2 activity (Diril et al., 2012)
Cdr2	correlates with attenuated hypoxia-inducible factor responses (Balamurugan et al., 2009)
Cxcr3	required for optimal differentiation of IFN-γ-secreting Th1 effector cells (Groom et al., 2012)
Cxcr5	mediates co-localization of effector Tfh cells and B cells in lymphoid organs during arthritis pathogenesis (Moschovakis et al., 2017)
Dusp14	regulates T cell proliferation and cytokine production (Yang et al., 2014)
Eea1	regulates the polarization of T cell and NK cell cytotoxic granules (Chiang et al., 2017)
Egr4	interaction with nuclear mediator NF-κB regulates the transcription of inflammatory cytokines (Wieland et al., 2005)
Fgf2	synergistically exacerbates tissue inflammation by regulating the production of cytokines and chemokines (Shao et al., 2017)
Foxm1	increases *Ube2c* transcription in glioma cells (Guo et al., 2017)
Il12rb2	modulates the differentiation of IFN-γ^+ Th1 effector cells (Bettelli and Kuchroo, 2005; Martínez-Barricarte et al., 2018)
Il13	mediates the expansion of Th2 cells (Deepak and Acharya, 2012; Scalzo-Inguanti and Plebanski, 2011)
Il1r2	negatively regulates IL-1 signaling (Peters et al., 2013)
Il9r	mediates Th17-driven inflammatory disease (Li et al., 2010; Nowak et al., 2009)
Kif4	suppresses the activity of DNA repair enzyme poly(ADP-ribose) polymerase-1 (Midorikawa et al., 2006)
Kpna2	regulates the expression of glycolytic genes downstream of effector-inducing mTORC1 (Chen et al., 2016)
Map3k8	activates mTORC1, promotes Th1/Th17differentiation, and suppresses iTreg differentiation (Acuff et al., 2015; Li et al., 2016)
Mir148a	controls Th1 cell survival by regulating Bim expression (Haftmann et al., 2015)
Mir150	cooperates with miR-150 to repress the expression of the Th17-promoting factor mTOR (Warth et al., 2015)
Mir183	enhances Th17 cell cytokine production and autoimmunity, and represses expression of the transcription factor Foxo1 (Ichiyama et al., 2016)
Mir21a	promotes Th17 differentiation by targeting and depleting SMAD-7, a negative regulator of transforming growth factor β (TGF-β) signaling (He et al., 2017; Murugaiyan et al., 2015)
Mir26a	downregulates Th17 and upregulates Treg cell function by targeting IL-6 (Zhang et al., 2015b)
Mir31	inhibits the induction of pTreg cells by suppressing Gprc5a (Zhang et al., 2015a)
Nkg7	upregulated by Th1-polarized T cells (Lund et al., 2005)
Nrp2	controls migration of T cell precursors (Mendes-da-Cruz et al., 2014)
Pdcd1	associated with Th cells in proliferative lupus nephritis (Caielli et al., 2019)
Plxnb2	required for normal germinal center humoral responses (Yan et al., 2017)
Ptger2	promotes differentiation and functions of Th1/Th17 cells (Boniface et al., 2009; Yao et al., 2009)
Ptpn3	regulates TCR signaling (Han et al., 2000; Sozio et al., 2004)

Gene	Function
Runx2	required for memory T cell persistence (Olesin et al., 2018)
Rgs16	regulates T cell activation and specific chemokine receptor-mediated migration (Lippert et al., 2003)
S1004	expression identifies memory $CD4^+$ T cells (Weatherly et al., 2015)
Shcbp1	regulates Th1/Th17 cell-mediated autoimmunity (Buckley et al., 2014)
Syk	activated in pathogenic $CD4^+$ T effectors (Chauhan et al., 2016; Krishnan et al., 2003)
Tjp2	interacts with SNX27 at the T cell immunological synapse (Tello-Lafoz et al., 2017) and regulates proliferation, cell size, and apoptosis (González-Mariscal et al., 2017)
Tnfsf4	promotes T cell survival, effector T cell phenotype, T cell memory, and reduction of regulatory function (Webb et al., 2016)
Ube2c	promotes phosphatidylinositol 3-kinase (PI3K)-Akt-mTOR pathway (Guo et al., 2017)
Uhrf1	regulates iNKT apoptosis and $Tbet^+$ iNKT1 effector frequencies (Cui et al., 2016)

KEY RESOURCES TABLE

REAGENT or RESOURCE	SOURCE	IDENTIFIER
Antibodies		
anti-CD11C	BioLegend	N418, RRID:AB_313773
anti-CD11b	BioLegend	M1/70 RRID: AB_312787
anti-CD8a	BioLegend	53–6.7 RRID: AB_312743
anti-B220	BioLegend	RA3–6B2 RRID: AB_312989
anti-CD49B	BioLegend	DX5 RRID: AB_313411
anti-CD25	BioLegend	PL61 RRID: AB_893288
anti-CD4	BioLegend	GK1.5 RRID: AB_312689 RRID: AB_312707
anti-CD45.2	BioLegend	104 RRID: AB_389211
anti-CD62L	BioLegend	Mel-14 RRID: AB_493719
anti-CD69	BD	H1.2F3
anti-IFNγ	BioLegend	XMG1.2 RRID: AB_315396 RRID: AB_315404
anti-CD3	BioLegend	145–2C11 RRID: AB_312669 RRID: AB_1877073
anti-Foxp3	eBioscience	FJK-16s RRID: AB_467575
anti-CD28	BioLegend	37.51 RRID: AB_312877
Fc-block (anti-CD16/32)	ATCC	2.4G2 (HB-197)
Streptavidin	BioLegend	N/A
anti-T-bet	BioLegend	4B10 RRID: AB_1595466
anti-RORγt	BD	q31–378 RRID: AB_2651150
anti-Ly-6C	BD	AL-21 RRID: AB_2737949
anti-CD5	BioLegend	53–7.3 RRID: AB_312733
anti-VISTA	BioLegend	MIH63 RRID: AB_2728190
anti-TCR V alpha 3.2	eBioscience	RR3–16
anti-TCR V beta 11	BD	RR3–15 RRID: AB_394704
anti-Nur77	BD	12.14 RRID: AB_395232
anti-PD-L1	BioXCell	10F.9G2 RRID: AB_10949073
Purified Rat IgG1, kappa isotype Ctrl antibody	BioLegend	RTK2071 RRID: AB_326508
Anti-Tri-Methyl-Histone H3 (Lys4) (C42D8)	Cell Signaling Technology	Rabbit mAb9751
Anti-Acetyl-Histone H3 (Lys27) (D5E4) XP®	Cell Signaling Technology	Rabbit mAb8173
Experimental Models: Organisms/Strains		
Mouse: C57BL/6J	Jackson Laboratory	Stock# 000664
Mouse: B6.SJL-*Ptprca Pepcb*/BoyJ	Jackson Laboratory	Stock# 002014
Mouse: *Foxp3*^{RFP} reporter	Jackson Laboratory	(Wan and Flavell, 2005)
Mouse: *Hopx*^{GFP} reporter	available at Jackson Laboratory on a mixed background	(Takeda et al., 2013)
Mouse: *Hopx*$^{-/-}$	available at Jackson Laboratory on a mixed background	(Shin et al., 2002)
Mouse: 2D2 TCR tg	Jackson Laboratory	(Bettelli et al., 2003)
Mouse: OTII TCR tg	Jackson Laboratory	(Barnden et al., 1998)
Mouse: *Rptor*$^{fl/fl}$	Jackson Laboratory	(Peterson et al., 2011)

REAGENT or RESOURCE	SOURCE	IDENTIFIER
Mouse: CD4-cre	Jackson Laboratory	(Lee et al., 2001)
Mouse: *Rag1*$^{-/-}$	Jackson Laboratory	(Mombaerts et al., 1992)
Cell line: A293	ATCC	N/A
Chemicals, Peptides and Recombinant Proteins		
Nutridoma SP	Millipore-Sigma	11011375001
Protein-G sepharose beads	GE Healthcare	17061801
Zombie Aqua Live/Dead viability dye	BioLegend	423102
Phorbol 12-myristate 13-acetate	Millipore-Sigma	P8139
Ionomycin	Millipore-Sigma	I0634
Pertussis toxin	List Biological Laboratories Inc.	180
Penicillin-streptomycin	Gibco	15140-122
Sodium Pyruvate	Gibco	11360-070
L-glutamine	Gibco	25030-081
HEPES	Gibco	15630-080
β-mercaptoethanol	Gibco	21985-023
Recombinant mouse IL-2	Biolegend	575406
Recombinant human TGF-β1	Biolegend	580704
TRIzol reagent	Invitrogen	15596026
Critical Commercial Assays		
Transcription Factor Staining Buffer Set	Invitrogen	00-5523-00
Fixation/Permeabilization Solution Kit	BD	554715
Mouse Th1/Th2/Th17 Cytokine Kit	BD Biosciences	560485
Streptavidin magnetic microbead	Miltenyi	130-048-101
mirVana miRNA isolation Kit	Invitrogen	AM1560
Eukaryotic RiboMinus Core Module v2	Life Technologies	N/A
Cell Proliferation Dye eFluor™ 450	Invitrogen	65-0842
Ion Total RNA-seq v2 kit	Life Technologies	N/A
cOmplete™, EDTA-free Protease Inhibitor Cocktail	Roche	N/A
Software and Algorithms		
TMAP (Torrent Mapping Program) aligner map4 algorithm	N/A	https://github.com/iontorrent/TMAP/blob/master/doc/tmap-book.pdf
R statistical computing	R Software	www.r-project.org
MATLAB®	The MathWorks	https://www.mathworks.com/downloads/
Gene Set Enrichment Analysis	Broad Institute, Inc.	ImmuneSigDB
BioMart	ENSEMBL	http://useast.ensembl.org
GraphPad Prism	Graphpad Software	https://www.graphpad.com
GSEA	UC San Diego, Broad Institute	https://www.gsea-msigdb.org/gsea/downloads.jsp
Bedtools	Quinlan and Hall, 2010	http://bedtools.readthedocs.io/en/latest/
Flowjo 9	FLOWJO, LLC	www.flowjo.com
Deposited Data		
RNA-seq and ChIP-seq data	This paper	NCBI GEO: GSE120277 and GSE141724